Quantitative Applications of ^{1}H and ^{31}P Chemically Induced Dynamic Nuclear Polarization

Inaguaraldissertation

zur

Erlangung der Würde eines Doktors der Philosophie

vorgelegt der

Philosophish-Naturwissenschaftlichen Fakultät

der Universität Basel

von

Dmytro Neshchadin

aus Odessa (Ukraine)

Basel, 2003

to Irina

and to my Parents

Acknowledgements

I would like to thank everyone who has contributed in any way into this study, helping me to undertake my research in Basel under pleasant, inspiring and liberal conditions. Special thanks and kindest regards to the following persons

Prof. Georg Gescheidt

for the amicable acceptance in his research group, openness and friendly guidance and supervision at the Physical Chemistry Institute of the University of Basel.

Dr. Günther Rist

for his remarkable introduction into CIDNP and NMR, optimism, moral support and inspirational response to my endless and sometimes not very clever questions.

Dr. Kurt Dietliker
Dr. Jean-Pierre Wolf
Dr. Jean-Luck Bierbaum
Dr. Martin Kunz

from CIBA SC for providing me exciting tasks for my research, chemicals, excellent and fruitful collaboration

Dr. Iwo Gatlik
Daniela Hristova

for their friendly collaboration within our research group

all my friends

Misha Pachkov, Olga Kondratieva, Simon Baeriswill, Sasha Kabanov, Zhenja and Tanja Sukhorukov for a lot of fun we had together during my unforgettable stay in Basel

Contents

List of Figures

List of Tables

Chapter 1

Introduction

Chemically Induced Dynamic Nuclear Polarization (CIDNP) spectroscopy has been widely used for many years for study of mechanisms of reactions that involve free radical pairs. Unlike Electron Spin Resonance (ESR) spectroscopy CIDNP provides an information on radicals that have been already reacted to paramagnetic species bringing the power of NMR into determination and identification of reaction pathways, yields and environmental effects. Since been discovered in year 1969 CIDNP was mostly applied in purely qualitative mechanistic studies where the simple rules developed by Kaptein allowed to deduce number of important reaction parameters. The quantitative application of CIDNP was rather difficult since there were sometimes no other experimental evidence to be compared especially within the cases where ESR failed. With the fast development of different theoretical calculation procedures which can provide rather precise knowledge on geometry, electron spin distribution and various magnetic properties of free radicals(g-factors, hyperfine coupling constants), CIDNP finds a new broad field of use especially where other physico-chemical methods are not successful by different reasons.

Being a variety of Nuclear Magnetic Resonance (NMR) spectroscopy CIDNP is limited by the same drawbacks - bad time resolution (usually microseconds) and poor sensitivity. Despite that it can follow the radical processes that are by far too fast to be observed ESR spectroscopy - the most straightforward method to observe

free radicals. The rate of fastest radical reactions that can be observed by CIDNP is determined by the rate of intersystem crossing which is about $10^{-10} - 10^{-9}$s. The information on free radical properties and properties of the paramagnetic products of the reaction is then stored within the longitudinal relaxation time of the particular nuclei which is typically 1 - 10s. That very important information includes spin distribution, radical concentration, rotation diffusion and magnetic properties of radicals and rates of reactions. Within the certain conditions it can be extracted by the analysis of CIDNP spectra.

The two different novel quantitative and semiquantitative applications of Chemically Induced Dynamic Nuclear Polarization combined with density functional quantum mechanical calculations and NMR studies are the subject of the present thesis. First application is of almost pure fundamental interest whereas the second finds its use in industry.

Chapter 2

Theoretical background

2.1 Chemically induced dynamic nuclear polarization

Spin populations of diamagnetic and paramagnetic species in the presence of the external magnetic field (NMR, ESR experiments), if no saturation and polarization transfer is present, are usually in thermal equilibrium (Boltzmann distribution). Chemically Induced Magnetic Polarization is the name given to the generation of the non-equilibrium nuclear and electron spin levels produced during chemical reactions with the participation of free radicals. The nuclear phenomenon is called Chemically Induced Dynamic Nuclear Polarization (CIDNP). That effect occurs when there is a selection (sorting) of nuclear spins. When such processes occur the NMR spectra is not anymore the conventional spectra with the respect to intensity of Zeeman transitions - a strongly enhanced emission or absorption could be observed - but still the same with the respect to chemical shifts of all observed NMR signals.

Two types of CIDNP effects are observed experimentally:

- **net effect**, when all the resonances of, in general, multiplet show either enhanced emission (E) or enhanced absorption (A).
- **multiplet effect**, when different polarizations within the multiplet are ob-

served. With the respect to the sequence of the emission or absorption transitions from lower field (higher chemical shift) to higher field (lower chemical shift) the patterns are defined as absorption/emission (A/E) or emission/absorption (E/A).

Sometimes both net and multiplet effects could be observed within the same multiplet. Figure 2.1 shows possible CIDNP effects for nuclei A in AX_3 spin system.

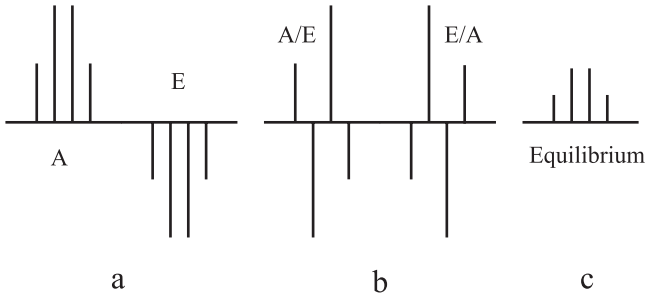

Figure 2.1: CIDNP effects on a quadruplet: a - net effects, b - multiplet effects, c - thermal equilibrium

The explanation of the experimentally observed CIDNP phenomena has been enabled with the appearance and development of Radical Pair Mechanism (RPM) theory.[1–5] The vast majority of the CIDNP observations can be treated within this theory. The RPM assumes the existence of a transient radical pairs in the reaction pathway. These radicals could be directly observed by ESR in certain favorable cases. On the other hand, in the NMR there are diamagnetic products of the reaction that are detected and all information about radical pair intermediates is obtained indirectly by the changes in the NMR signal intensities of the products. During past 30 years RPM theory was modified by various authors but the fundamental ideas were not changed, and most CIDNP experiments could be treated not only qualitatively (reaction pathways) but also quantitatively (rate constants, reaction yields, magnetic parameters, liquid dynamics). The complete description of CIDNP origin and implementation is given in few major monographs[6–8] and diverse reviews.[9–20]

2.2 Radical pair mechanism theory

The main idea of Radical Pair Mechanism is that in the presence of external magnetic field the CIDNP effect is due to a nuclear spin dependent recombination probability, *i.e.* the probability for two radicals to react (recombine, disproportionate) depends on the nuclear spin states of those two radicals. If the external magnetic field (H_0) exists, the precursor molecule (R_1-R_2) is cleaved into two radicals $R_1\cdot$ and $\cdot R_2$ with the correlated electron spins, this is called radical pair. During the thermal cleavage singlet radicals pairs (S) are formed predominantly[a], whereas photochemical process leads to triplet radical pairs. In the magnetic field triplet state is split into three sublevels T_1, T_0 and T_{-1}. When the two radicals are enough far apart the singlet S and triplet T_0 states are degenerate, at the relatively small inter-radical distances (r) the singlet and triplet states possess different energies because of high exchange interaction J(r) as shown on Figure 2.2.

Due to Brownian motion, the relative separation of the two radicals becomes time dependent. If one assumes that the total spin state of the system is not altered during the time in which the two radicals are in contact (*i.e.* r<r* on Figure 2.2) then the system "follows the energy curves", *i.e.* the energy of the system is represented by the stationary energy for any distance. Systems in triplet state thus experience a repulsive force for all short distances (r<r*), and the triplet state is anti-bonding. On the other hand, two radicals in the singlet state will experience an attractive force for distances down to r=d where a strong repulsive force states in. If the depth of the potential well at r=d is larger than a kT then the radicals become trapped and thus they have reacted. In the following it is assumed that only singlet pairs can react which is by far the most common case.

The observation of CIDNP effects require triplet-singlet interconversion. Mixing of the singlet and triplet states may be caused by differences in Zeeman and hyperfine interactions and could be illustrated by vector representation on Figure 2.3. On

[a] there are cases where thermal cleavage happens in the triplet electronic state, whereas photochemical cleavage occurs from the singlet one

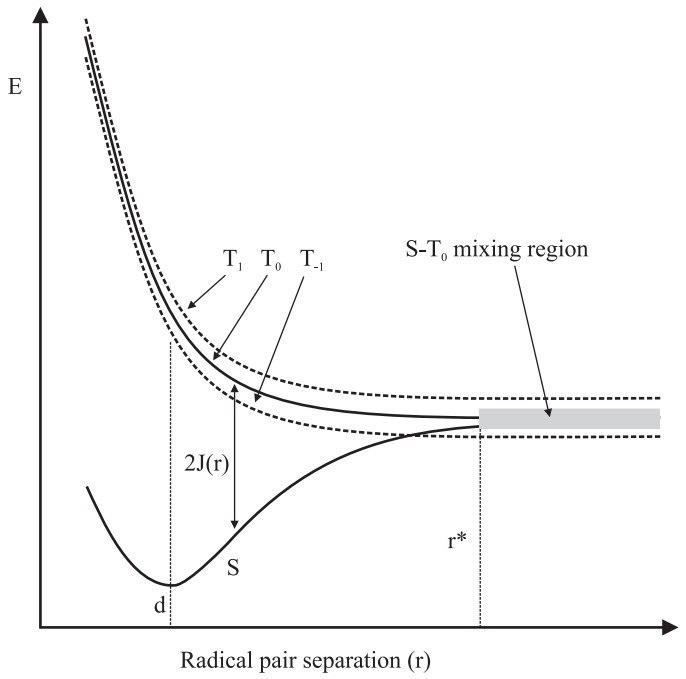

Figure 2.2: Energy level diagram of a separating radical pair in an external magnetic field (H_0) as a function of inter-radical distance (r)

Figure 2.3 the radical pair is formed in triplet state then it undergoes the diffusion "excursion". After radical pair is being separated to a certain distance r>r* where the exchange interaction J(r) is small enough each electron spin starts to precess independently with the different frequencies that leads to transition from T_0 to S state[b]. The rates of precession of two electron spins differ since they experience different magnetic fields[c]. The difference between Larmor frequencies of two electron spins is given by the following equation[21]:

$$\Delta\omega = \omega_1 - \omega_2 = \frac{1}{2}\left[\mathrm{H_0}\Delta\mathrm{g}\beta_e\mathrm{h}^{-1} + \sum_{i=1}^{n}\mathrm{a}_{1i}\mathrm{m}_{1i} - \sum_{j=1}^{k}\mathrm{a}_{2j}\mathrm{m}_{2j}\right]^{\mathrm{d}} \tag{2.1}$$

[b]Transition from T_{-1} and T_1 to S is spin forbidden but can occur through the T_0 state

[c]This is true for radical pairs that consist from nonequivalent radicals

[d]Equation is valid within the frame rotating with the frequency $\frac{1}{2}\Delta\omega$; ω_1 and ω_2 - Larmor frequencies of unpaired electron spin of R_1 and R_2, H_0 - strength of magnetic field, Δg - difference of g-factors of radical R_1 and R_2, β_e - Bohr magneton (9.2741×10^{-24} A m^2), a_{1i} and m_{1i}, a_{2j} and

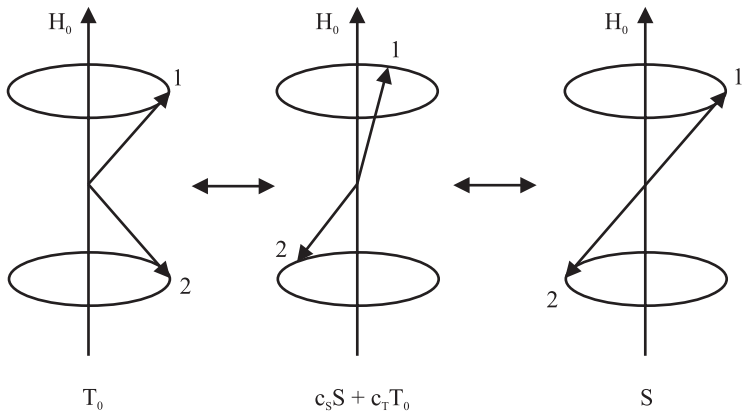

Figure 2.3: Vector representation of S-T_0 mixing of electron spins 1 and 2 (c_S+c_{T_0}=1).

The first term of equation arises from the spin-orbit interaction; g-factor is related to spin-orbit coupling of odd electron and therefore to spin-orbit induced magnetic fields experienced by radical R_1 and R_2. The second and third terms are responsible for the electron-nuclear coupling(the hyperfine splitting in ESR). Electron-spin interaction also contributes to local fields affecting two radicals. Assuming for simplicity the radical pair formed in T_0 state in which only one radical carries the magnetically active nuclei with $|m_{1i}|=\frac{1}{2}$, $\Delta g>0$, $a_{1i} > 0$. For such a pair there are two possible values of $\Delta\omega$ depending on the spin orientation according to the external magnetic field($m_{1i} = \pm\frac{1}{2}$):

$$\alpha, m_{1i} = +\frac{1}{2}, \qquad \Delta\omega_+ = \frac{1}{2}\left[H_0 \Delta g \beta_e h^{-1} + \frac{1}{2} a_{1i}\right] \tag{2.2}$$

$$\beta, m_{1i} = -\frac{1}{2}, \qquad \Delta\omega_- = \frac{1}{2}\left[H_0 \Delta g \beta_e h^{-1} - \frac{1}{2} a_{1i}\right] \tag{2.3}$$

This states that the rate of S-T_0 mixing, which is proportional to $\Delta\omega$, depends on the nuclear spin orientation. This is the main idea of Radical Pair Mechanism theory. If $\Delta\omega_+ < \Delta\omega_-$ then radical pairs with α spin orientation reach singlet state faster and react to products with overpopulated lower magnetic state. That will

m_{2j} - hyperfine coupling constant and magnetic quantum number of nuclei i and j in radical R_1 and R_2 correspondingly

rout to enhanced absorption in CIDNP spectra. Consequently, radical pairs with nuclei in β spin state would possess longer lifetime and thus have higher probability to escape from the solvent cage and form paramagnetic species with excess of β-spin nuclei giving rise to enhanced emission in CIDNP experiment. Products formed by recombination of initial radical pair are called "cage products" (also recombination products), compounds formed by escaping from cage are called "escape products". Enhanced absorption/emission is called CIDNP polarization. Polarizations from cage and escape products always have opposite signs (Figure 2.4). Fast S-T_0 mixing enhances the probability to recombine for initially triplet pairs and reduces it for singlet ones. Slow mixing does opposite.

When the radical pair is formed in the singlet state the higher difference between Larmor frequency would lead to the faster S-T_0 mixing and that is why enhance the probability to escape. The slow rate of S-T_0 mixing will do opposite.

The generation of CIDNP polarization is rather fast process that takes $10^{-10} - 10^{-7}$s. However, non-equilibrium spin population is preserved within the longitudinal relaxation time of observed nuclei (0.5 - 10s for protons in small molecules) and could be observed with rather long (0.5-4 μs) radiofrequency pulses. The upper limit of CIDNP observation is determined by the short relaxation times in paramagnetic species (10^{-3}s), if the lifetime of the radical pair is considerably longer the initially generated polarization vanishes.

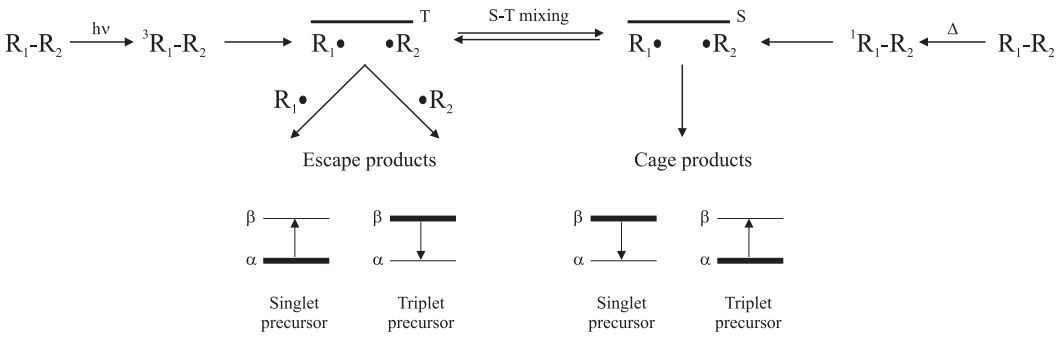

Figure 2.4: Representation of the processes involved into RPM of CIDNP.

Kaptein has formulated simple rules[22], for a qualitative interpretation of CIDNP spectra:

- **net effect** (Γ_{ne}):

$$\Gamma_{ne} = \mu\ \varepsilon\ \Delta\mathrm{g}\ \mathrm{a}_i \tag{2.4}$$

- **multiplet effect** (Γ_{me}) of a nucleus i coupled to nucleus j:

$$\Gamma_{me} = \mu\ \varepsilon\ \Delta\mathrm{g}\ \mathrm{a}_i\ \mathrm{a}_j\ \mathrm{J}_{ij}\ \delta_{ij} \tag{2.5}$$

where the signs are according the following:

μ	+	triplet precursor
	–	singlet precursor
ε	+	cage products(recombination, disproportionation)
	–	escape products
Δg		sign of g_1-g_2, where g_1 is the g-factor of the radical where nucleus interest is located
a_i		sign of the hyperfine coupling constant of nucleus i
a_j		sign of the hyperfine coupling constant of nucleus j
J_{ij}		sign of the nuclear coupling constant between nuclei i and j
δ_{ij}	+	when nuclei i and j are on the same radical
	–	when nuclei i and j are on different radicals
Γ_{ne}	+	absorption (A)
Γ_{ne}	–	emission (E)
Γ_{me}	+	emission/absorption (E/A)
Γ_{me}	–	absorption/emission (A/E)

Those rules allow to explain and predict signs of CIDNP polarizations or to extract any variable if all others are known in the case when $\Delta g H_0$ is considerably larger than

the hyperfine coupling constant. Kaptein's rules certainly have some restrictions and can be violated when $\Delta g H_0$ is comparable or even smaller than hyperfine coupling constant.

2.3 Quantum mechanical description of CIDNP

The spin Hamiltonian that describes the intersystem crossing in radical pair can be obtained from total Hamiltonian in the case of near degeneracy of S and T states. According to perturbation procedure the effective spin Hamiltonian of radical pair consisting from terms appropriate to the S and T states and terms connecting these states is:

$$\widehat{H}_{RP} = \widehat{H}_{ex} + \widehat{H}_{ze} + \widehat{H}_{hf} + \widehat{H}_{d} \tag{2.6}$$

where $\widehat{H}_{ex}$ describes exchange interaction, $\widehat{H}_{ze}$ - Zeeman interaction, $\widehat{H}_{hf}$ - hyperfine interaction and $\widehat{H}_{d}$ - electron dipolar coupling. Expanding all the terms will lead to the following representation of $\widehat{H}_{RP}$:

$$\widehat{H}_{RP} = \widehat{H}^0 + \widehat{H}' \tag{2.7}$$

where

$$\widehat{H}^0 = \frac{1}{2}\Delta g \beta_e h^{-1} H_0 (S_{1z} + S_{2z}) - J(\frac{1}{2} + 2\widehat{S}_1 \cdot \widehat{S}_1) + \\ + \frac{1}{2}(\widehat{S}_1 + \widehat{S}_1)(\sum_{i=1}^{n} a_{1i}\widehat{I}_{1i} + \sum_{j=1}^{k} a_{2j}\widehat{I}_{1j}) \tag{2.8}$$

$$\widehat{H}' = -\frac{1}{2}\Delta g \beta_e h^{-1} H_0 (S_{1z} - S_{2z}) + \\ + \frac{1}{2}(\widehat{S}_1 - \widehat{S}_1)(\sum_{i=1}^{n} a_{1i}\widehat{I}_{1i} - \sum_{j=1}^{k} a_{2j}\widehat{I}_{1j}) \tag{2.9}$$

[e] the solution of time dependent Schroedinger equation $i\partial\phi/\partial t = \widehat{H}_{RP}\phi$ in the basis of χ_n nuclear spin product functions[f] leads to the probabilities to find radical pair in either triplet or singlet state and thus to react. Starting from triplet precursor

[e] $\widehat{S}_1$ and $\widehat{S}_2$ are electron spin operators, S_{1z} and S_{2z} are their projections on the direction of the magnetic field (axe z), $\widehat{I}_{1j}$ and $\widehat{I}_{2j}$ - nuclear spin operators, J - exchange integral

[f] $\phi_n = [c_{Sn}(t)S + c_{Tn}(t)T_0]\chi_n$

(photocleavage, $c_{Sn}(0) = 0, c_{Tn}(0) = 1$) we will have the following probability to of finding radical pair in singlet state:

$$|c_{Sn}^{T}(t)|^2 = \left(\frac{\Delta\omega_n}{(J^2 + \Delta\omega_n)^{1/2}}\right)^2 \sin^2 (J^2 + \Delta\omega_n)^{1/2} t \tag{2.10}$$

$\Delta\omega_n$ is the already treated difference of Larmor frequencies for the particular nuclear spin state n. It is obvious that big values of the exchange integral J (small inter radical distances) will make the probability of $|c_{Sn}^{T}(t)|^2$ very small - intersystem crossing and therefore observation of CIDNP unprobable. Finally quantum mechanical treatment gives the following expression for the CIDNP polarization for the $n \rightarrow m$ transition for the nuclei residing on the radical R_1

$$I_{nm} \propto \langle \Delta\omega_n^2 - \Delta\omega_m^2 \rangle =$$

$$= \frac{1}{2} \mathrm{a}_{1i} \left\langle \Delta \mathrm{g} \beta_e \mathrm{H}_0 \mathrm{h}^{-1} + \sum_{i=1}^{n} \mathrm{a}_{1i} \mathrm{m}_{1i} - \sum_{j=1}^{k} \mathrm{a}_{2j} \mathrm{m}_{2j} + \mathrm{a}_{1i} \left(\mathrm{m}_i - \frac{1}{2} \right) \right\rangle \tag{2.11}$$

the first term in the right part of the equation 2.11 gives rise to the net effect, emission or absorption depending on the sign of $\Delta \mathrm{g a}_{1i}$, second and third to multiplet effect of nuclei in radical R_1 and coupled to it nuclei in radical R_2. The forth and the last term do not play any role in the first order NMR spectra(for details see [23, 24]).

For the the nuclei with the magnetic quantum number $\frac{1}{2}$ assuming that NMR transitions are proportional to longitudinal relaxation time and there are no multiplet and second order effects present equation 2.11 gets:

$$I = \mathrm{C\ P\ T_1} \left[\sqrt{\left| \Delta \mathrm{g H_0} + \frac{1}{2} \mathrm{a} \right|} - \sqrt{\left| \Delta \mathrm{g H_0} - \frac{1}{2} \mathrm{a} \right|} \right] \tag{2.12}$$

where P is the proportionality constant characteristic for every radical pair and dependent on solvation, temperature and diffusion properties, C - absolute radical concentration. The polarization intensity I as the function of the hyperfine coupling constant a is shown in figure 2.5. The function was calculated for $\Delta\mathrm{g} = 0.002$, P=1, C=1, $\mathrm{H_0}$=4.7 T that corresponds to 200 MHz NMR magnet. It is obvious that in

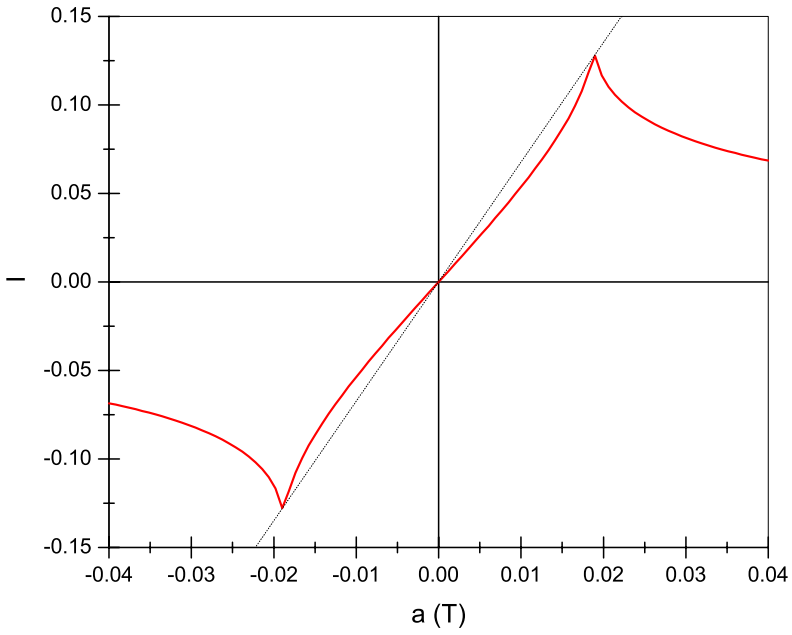

Figure 2.5: Calculated intensity of CIDNP polarization vs. hfc a

the range from -20 to 20 mT CIDNP intensity is very well approximated by the linear function

$$I(a) = C\ P\ \ T_1\ a \tag{2.13}$$

Chapter 3

Experimental

3.1 Description of the equipment

^{1}H-, ^{31}P-NMR and CIDNP spectra were recorded on Bruker AM 200 MHz and Bruker AVANCE DPX 200 MHz spectrometers with the wide bore superconducting magnet (4.7 Tesla) using interchangeable ^{1}H-5mm and ^{31}P-5mm CIDNP probeheads. The quartz prisms allowed the irradiation of the sample during the acquisition of CIDNP spectra. Arrangement of probeheads and block diagram of the instrumentation are shown on Figures 3.1 and 3.2 correspondingly.

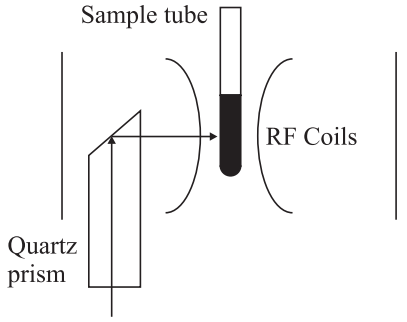

Figure 3.1: Arrangement of probeheads

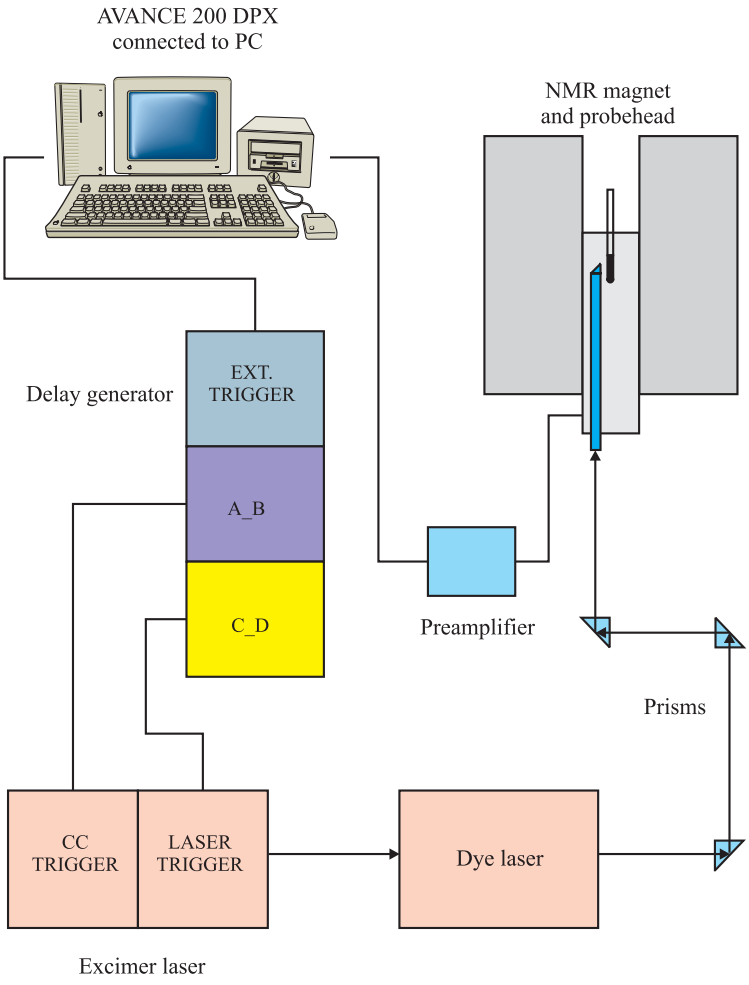

Figure 3.2: Block diagram of the equipment

The irradiation was performed by Lambda Phisik dye laser FL 3001/2 pumped by a Questek 2000 excimer laser with the pulse duration of about 10-20 ns. The excimer laser operates with XeCl which emission lies at 308 nm. The gas mixture consisting of 80 mbar of HCl, 80 mbar of Xe and 2840 mbar of Ne was found to be optimal in terms of energy, stability and durability. The 1,4-dioxan dye solution based on PTP (p-terphenyl, LC 3400) has provided the needed light output at 342.5 nm. Concentration of PTP in the oscillator cavity was 0.24 g/l while in amplifier only 0.08 g/l. The conversion efficiency of the dye laser lies in the range of 5-8% depending on the alignment of the optics and decomposition of the dye solution.

Output energy after the dye laser was of about 6-10 mJ/pulse with the input of 200 mJ/pulse from excimer. Excimer laser has been trigged by the Stanford Research DG 535 pulse/delay generator. The laser beam going from the dye laser was directed *via* prisms into the flat bottom of the quartz rod and further into the probehead reaching the sample in the middle of receiver coils. The diameter of laser beam inside the probehead has been about 2-3 mm. Rough control of the laser alignment have been done by photosensitive paper.

3.2 CIDNP experiments

Figure 3.3 shows a pictorial representation of CIDNP experiment in time domain, where SAT denotes either a broadband or composite pulse presaturation for ^{1}H-CIDNP or a sequence of 180° radio-frequency pulses for ^{31}P-CIDNP which served to suppress regular NMR intensities. LP - one or several laser pulses, RF - radio-frequency pulse, which must be in the range of 10-30° and AQ represents acquisition. t_1, t_2 are variable time delays, t_L - duration of laser pulse/pulses, t_D=t_1 + t_2 + t_L.

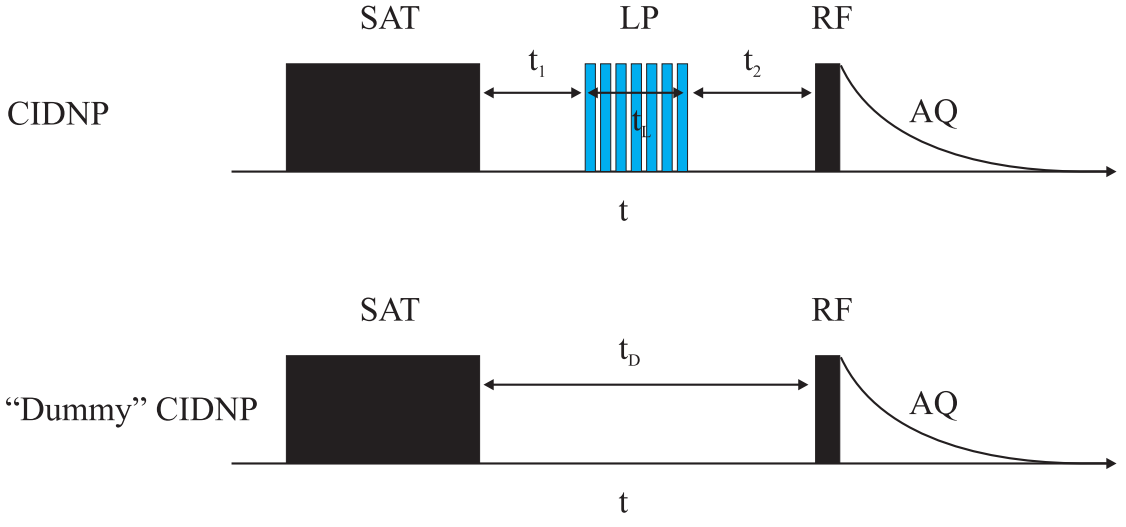

Figure 3.3: Timing of CIDNP and "dummy" CIDNP experiments

Most of ^{1}H-, ^{31}P-CIDNP spectra were recorded with the help of automation programs written on the internal Aspect 3000 and AVANCE DPX script languages. The MUTRISAT.AU and CIDNP-31P.AU programs were applied to carry out ^{1}H-, ^{31}P-CIDNP experiments correspondingly.

The above mentioned automation programs are shown below:

MUTRISAT.AU

```
;beginning of program
1   DO                  ;zero memory
2   D1 BB S1            ;broadband decoupling with the power S1
3   D2 DO               ;decoupler off
4   D3                  ;delay between decoupler off and laser trigger
5   P2:C4               ;laser trigger
6   D4                  ;delay between the laser pulses
7   LO TO 5 TIMES X     ;loop to 5 times X
8   D5                  ;delay between the last laser pulse and RF pulse
9   GO=2                ;start NMR program and loop to 2
10  EXIT                ;end of program
```

CIDNP-31P.AU

```
;beginning of program
;zgdc
;avance version
;1D sequence with presaturation

# include Avance.incl
"d11=30m"
```

```
"d1=30m"
1 ze
d11 pl12:f2
d11 cpd2:f2
2 d1
3 10000u
HS_ON
d10
HS_OFF
lo to 3 times X
p1*0.33 ph1
go=2 ph31 wr #0
d11 do:f2
exit

ph1=0 2 2 0 1 3 3 1
ph31=0 2 2 0 1 0 1 3 3 1

;pl1 : f1 channel - power level for pulse (default)
;pl12: f2 channel - power level for CPD/BB decoupling
;p1 : f1 channel - high power pulse
;d1 : relaxation delay; 1-5 * T1
;d11: delay for disk I/O [30 msec]
;cpd2: decoupling according to sequence defined by cpdprg2
;pcpd2: f2 channel - 90 degree pulse for decoupling sequence
;end of program
```

The parameters used in ^{1}H-, ^{31}P-NMR and CIDNP experiments are shown in Table 3.1

Table 3.1: Set up parameters for NMR and CIDNP experiments (Aspect 3000, AVANCE DPX)

Parameter	^{1}H-NMR	^{1}H-CIDNP	^{31}P-NMR	^{31}P-CIDNP
FQ (MHz)	200.13	200.13	80.015	80.015
SW (Hz)	4000	4000	18000	18000
PW (deg)	80°	80°	30-40°	30-40°
RD (s)	0	0	2-4	0
D1 (s)	-	3	-	0
D2 (s)	-	2	-	0
D3 (μs)	-	2	-	2
D4 (ms)	-	6	-	6
D5 (μs)	-	2	-	2
P2 (μs)	-	3	-	3
P9 (CPD)	-	-	100	100
X	-	5-10	5-20	5-20
P20 (deg)	-	-	-	180°
D20 (ms)	-	-	-	50
L1	-	-	-	100-300

Waltz16 pulse sequence (QqqQ, Q=270_{-x} - 360_x - 180_{-x} - 270_x - 90_{-x} - 180_x - 360_{-x} - 180_x - 270_{-x}, q=270_x - 360_{-x} - 180_x - 270_{-x} - 90_x - 180_{-x} - 360_x - 180_{-x} - 270_x) has been used as the composite pulse decoupling program (cpdprg2) for presaturation of ^{31}P as well as for the decoupling of phosphorus from protons. Synchronization of the spectrometers, both Aspect 3000 and AVANCE 200 DPX, with the excimer laser has been carried out through the homospoil output (HS_ON/HS_OFF) of the corresponding console.

The number of laser pulses X and delay between the laser pulses for CIDNP experiments were chosen such that the formation of radical pairs was high enough and that nuclear spin relaxation before the observing radio-frequency pulse was not significant.

Triggering of the excimer laser was done through the Stanford Research DG 535 pulse/delay generator. The following delay times have been used:
A = 0.0 ms
B = 0.1 ms
C = 4.0 ms
D = 4.1 ms
Output channels pulse generator which were used are A_B and C_D, for CC trigger and laser trigger correspondingly.

Tetramethylsilane ($Si(CH_3)_4$) was used as an internal standard for ^{1}H-NMR and CIDNP measurements, while $H_3PO_4$was a reference in ^{31}P experiments (positive values indicate shift to a lower field).

500 W high pressure mercury lamp with the external water cooling was used for some polymerization experiments as the irradiation source.

3.3 Quantitative CIDNP and NMR measurements

Quantitative determination of species by Nuclear Mgnetic Resonance methods is possible only via comparison with the known quantity of reference standard. In order to have such a reference for quantitative measurements, spectra using CIDNP pulse sequence but without laser irradiation ("dummy" CIDNP) Figure 3.3 were always recorded. To avoid intensity distortion due to signal enhancement in CIDNP experiments, the receiver gain (rg parameter for both Aspect and AVANCE) was reduced by the factor 2 compared to one that was found to be optimal for "dummy" measurements. This allowed to avoide reciever overmodulation by very strong CIDNP polarizations.

After phase and baseline correction the particular signal of interest was fitted with the Gaussian function

$$F(x) = A_0 exp(-\frac{(x-x_0)^2}{2w^2}) \tag{3.1}$$

where A_0 is the amplitude of the signal, x_0 - center of the signal (resonance frequency). $w = \frac{w_1\sqrt{ln4}}{2}$ where w_1 is the width of the signal at the half height. Produced function was integrated from $x_0 - 4w_1$ to $x_0 + 4w_1$:

$$\int_{x_0-4w}^{x_0+4w} F(x) = A_0 w\sqrt{\pi}\sqrt{2} erf(2\sqrt{2}) \tag{3.2}$$

where erf is error function which is defined for all complex x by:

$$erf(x) = \frac{2}{\sqrt{\pi}} \int_0^x exp(-t^2)dt \tag{3.3}$$

and equals 0.999 in our case.

Deduced integrals have been used as the integral intensities of the NMR and CIDNP transitions. The difference between the integral intensities of polarized NMR signal and NMR signal in "dummy" spectra were assumed to be estimates for CIDNP polarizations. The example of CIDNP polarization calculation for typical ^{31}P-CIDNP spectrum of TPO (diphenyl(2,4,6-trimethylbenzoyl)phosphine oxide) is shown on Figure 3.4. I_d and I_p denote the integral intensities of the same NMR

transition in "dummy" and polarized spectra correspondingly; I_{CIDNP} is the observed CIDNP polarization. All calculations were made using the absolute mode of the spectrometer and no windowing function were applied. The phase correction of CIDNP spectra in every particular case was exactly the same as of corresponding "dummy" CIDNP.

Calibrations of the laser beam energy inside CIDNP probehead were done using the reference ^{31}P-CIDNP spectra of TPO; observed CIDNP polarizations of the latter have been used as the normalization coefficients in all subsequent CIDNP measurements.

Longitudinal relaxation times (T_1) of ^{1}H and ^{31}P nuclei have been measured by the standard inversion recovery experiment upon the conditions of subsequent quantitative CIDNP experiments. For each observation of (T_1) at least 10 data points were monitored. Experimental error was found to be less then 2%.

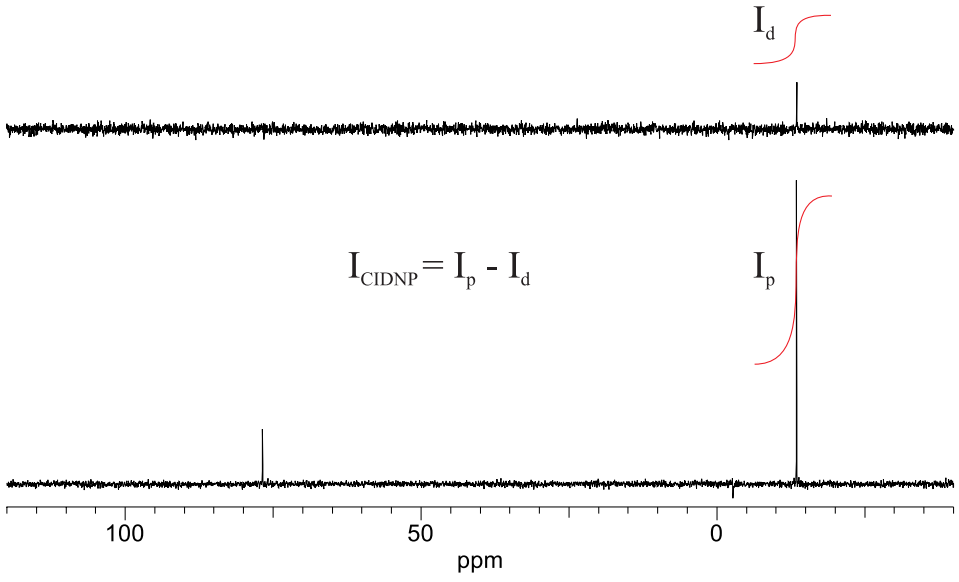

Figure 3.4: Calculation of CIDNP polarizations

3.4 Sample preparation

Pyrex sample tubes with the internal diameter of 5mm, obtained from Wilmadlabglass(USA) were used. Hydrocarbon cage compounds were synthesized, characterized and purified in the group of Prof. Horst Prinzbach (University of Freiburg, Germany). Phosphine oxide photoinitiators were prepared by Ciba SC (Basel Switzerland). Hydrocarbon cages were dissolved in deuterated dichloromethane (CD_2Cl_2, Cambridge Isotope Laboratories, Inc.), Photoinitiators - in deuterated benzene (C_6C_6, Dr. Glaser AG) in concentrations 0.005 mol/dm^3 and 0.025 mol/dm^3 correspondingly. Hydrocarbon samples were deoxygenated by bubbling of argon during 10 min. Phosphine oxides have been used without any additional treatment in order to simulate industrial conditions.

3.5 Quantum mechanical calculations

Quantum mechanical calculations were done using Gaussian 98 Rev.A.7 software package. Both geometry optimization and single point calculations have been performed by Beke3LYP method using 6-31G(d) basis set, which was found to be optimal in terms of cost and reliability. The header of the typical input file for QM calculation of phosphinoyl radical is shown below:

%chk=

#opt ub3lyp/6-31g(d) gfprint density=current pop=full test

Title card

0 2

Chapter 4

Restricted hydrocarbon cages

The most straightforward method to determine and characterize free radicals is ESR (Electron Spin Resonance). It possesses high sensitivity(sometimes 1000 times higher then NMR) and provides a unique information on free radical structure which is mirrored by the spin distribution. However it does have some limitations with the respect to the persistence/stability of the radicals which can be detected. In contrast to ESR the CIDNP observes only a diamagnetic species that were formed through the interaction of the free radicals. Although the time resolution of the NMR-based CIDNP experiments is rather poor compared to ESR, the shortest lifetime of the radical pair that can be indirectly characterized is limited only by the rate of the singlet-triplet mixing of those pairs. That rate depends on hyperfine coupling

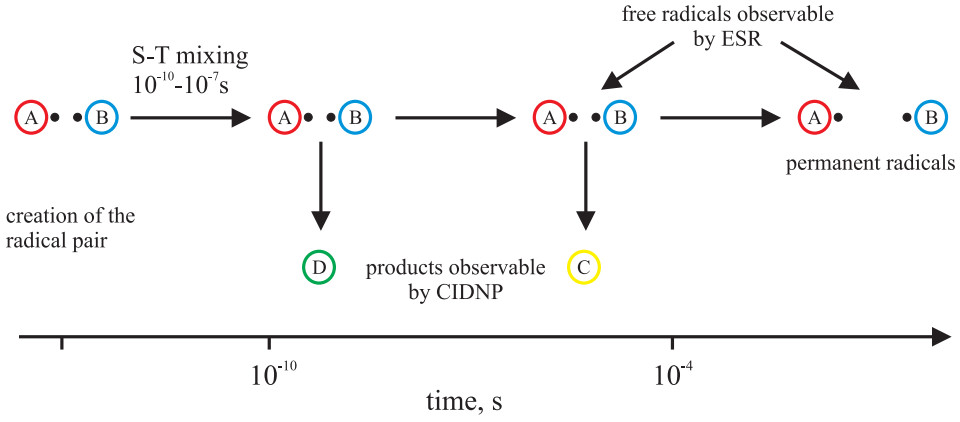

constant, difference of g-factors of radicals, external magnetic field and exchange interaction. All that means that at certain conditions the lifetime of the radical pair should be slightly longer than 10^{-10}s to give rise to CIDNP polarization what is by far too fast for CW ESR.

In this chapter we present the application of ^{1}H-CIDNP for determination and characterization of species that have not been evaluated by CW ESR even at low temperature in frozen matrix.

4.1 Compounds investigated

Cyclobutanoid radical cations (four-center/tree-electron systems, 4c/3e-systems) have been under extensive investigation for some time. A number of experimental[25–27] and theoretical[28–31] studies had been carried out. The reason for such an interest in those systems is based on the idea that they can serve as an illustrative models of the interface between theory and experiment.

The four-membered ring institutes a structure that differs significantly from the ideal tetrahedral arrangement that is postulated for the sp^3 hybridized carbon atom. The parent strained cyclobutane has a ring structure of a D_{2d} symmetry. A number of theoretical investigations were directed towards the structural properties of the cyclobutane mono-cation. That cation is evidently very reactive and thus could be observed, for example by ESR, only in frozen matrices after γ or X-ray irradiation. The intriguing features of 4c/3e-systems are the two minima of the reaction coordinate calculated for the synchronous, symmetry forbidden[32] [2+1] cycloaddition of ethylene to ethylene radical cation with the imposed D_{2h} symmetry.(Figure 4.1[33]) Neither the "extended"(π-complex, r≈2.6Å) nor the "tight"(cyclobutane-like, r≈1.75Å) configuration is the true minimum. Without the extra stabilization, both structures tend to open into a linear tetramethylene radical cation.[34] The rigid molecular skeletons can provide additional balance to 3e/4c-radical cations and indeed they do so, but even extra stabilized species are not easy to detect and characterize by the conventional methods used for the studies of free radical.

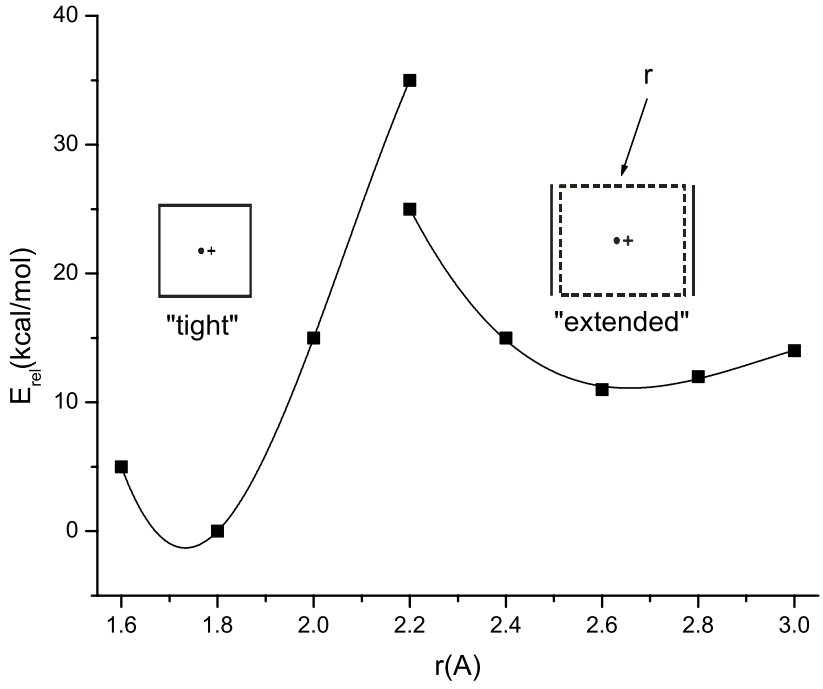

Figure 4.1: Calculated reaction coordinate for the [2+1]cycloaddition of ethylene to the ethylene radical cation with D_{2h} symmetry. Energies are calculated at the PMP2/6-31G* level of theory and are relative to the minimum structure "tight".[33]

The main feature of all pagodanes and their 90°-"twisted" analogues iso-pagodanes is the four carbon center planar moiety, in general, of different symmetry that resides in the center of molecule. Despite the very strained structure, pagodanes and iso-pagodanes are very stable thermally. For example, [2.2.2.2]pagodane (**P3**) melts unchanged at 213°C[35].

Rigid carbon skeleton of pagodanes and iso-pagodanes should bring the stabilization needed to make their 3e/4c radical cations observable and even distinguishable in both isomers "tight" and "extended". That could probably shed the light on the "mystery" of cyclobutane radical cation. Apart from being the sub-

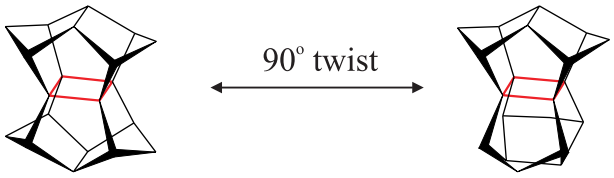

ject of pure theoretical interest, pagodanes and their analogs iso-pagodanes were recently introduced as the intermediates in the direct and versatile synthesis of various dodecahedranes[36–38] - the so called "pagodane route" developed by the research group of Prof. H.Prinzbach at University of Freiburg(Germany).

All compounds studied by ^{1}H-CIDNP and chemical shifts of their protons are shown on figure 4.2. The assignment of NMR transitions was done according to Exner[39] and Etzkorn[40] from Freiburg University (Germany) who have synthesized the studied compounds. The oxidation of investigated compounds was done photochemically by chloranil(tetrachloro-1,4-benzoquinone, $C_6O_2Cl_4$). Chloranil possesses significant absorption at 342.5 nm and quite high electron accepting ability (ε_{342}=780 mol^{-1}cm^{-1}, reduction potential +0.02 V *vs.* SCE [41]) in the excited triplet state. Chloranil was successfully used as electron acceptor for the photochemical oxidation in CIDNP studies of numerous compounds[42–45]. Also, the magnetic properties of chloranil radical anion, that is formed after chloranil reduction, are very well known.[46]. Moreover tetrachloro-1,4-benzoquinone does not carry any protons and does not interfere with ^{1}H-NMR and CIDNP spectra of pagodanes.

4.2 Previous studies

Highly persistent (2 days, at 20°C) 4-center-3-electron radical cation was registered by ESR upon electrochemical oxidation of [1.1.1.1]pagodane (**P1**)[47]. This finding has triggered numerous studies[48–50], mostly ESR and cyclovoltometric, on differently modified related skeletons: [2.2.1.1]pagodane (**P2**) and [2.2.1.1]isopagodane[51], [1.1.1.1]pagodane (**P1**) and [1.1.1.1]isopagodane[33, 52, 53], [2.2.2.2]pago-

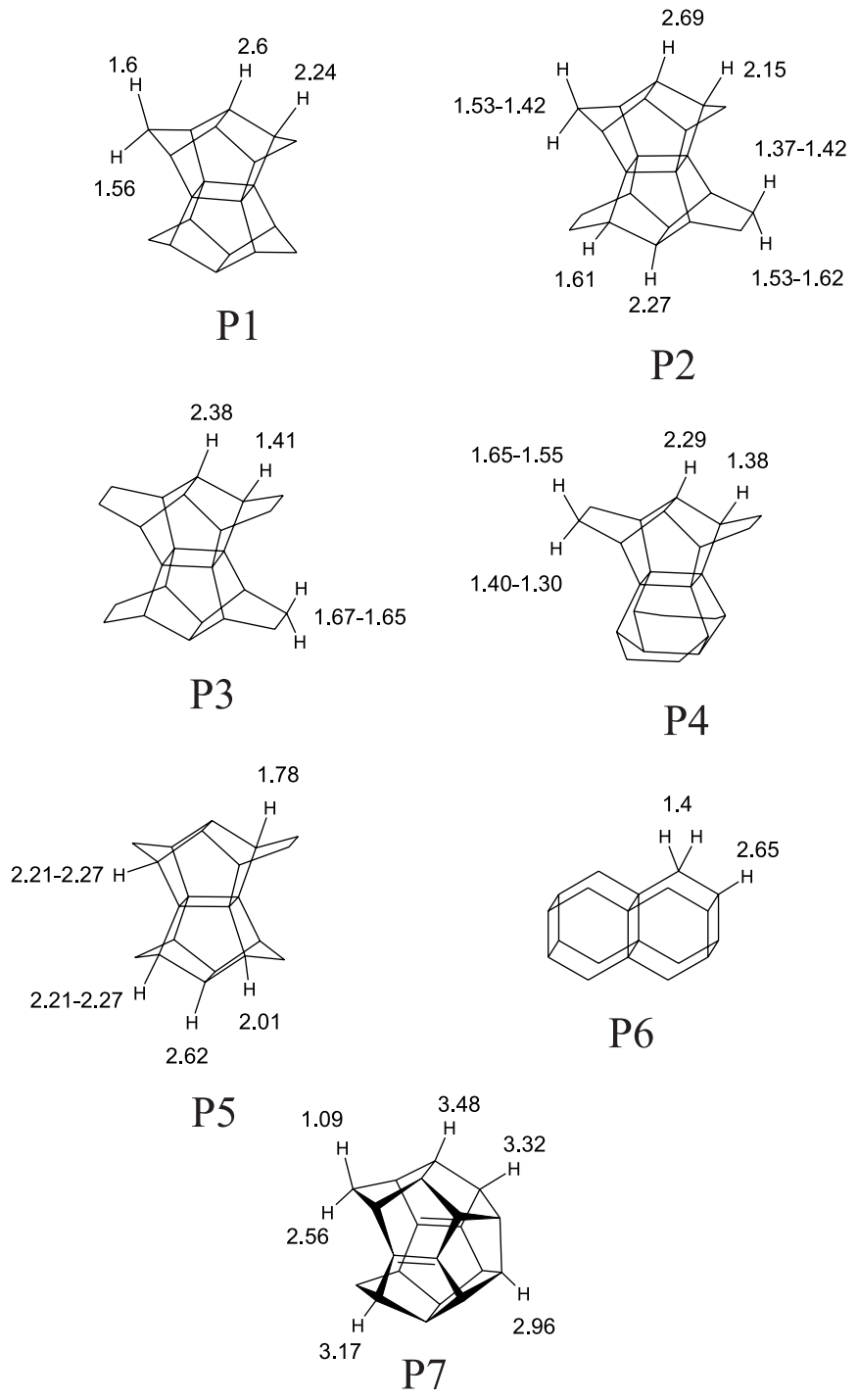

Figure 4.2: Compounds investigated and chemical shifts of important protons(ppm, according to TMS).

dane (**P3**)[35]. Significant differences with respect to stability persistence and chemical transformations (Figure 4.3) of the corresponding radical cations have been es-

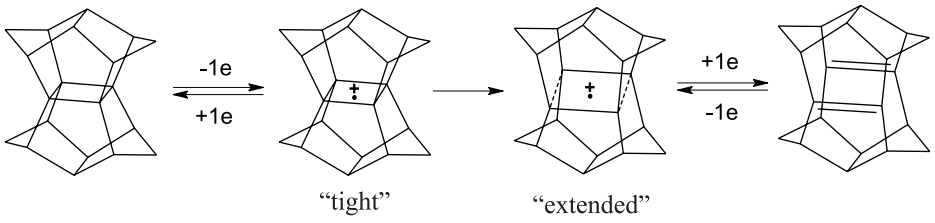

Figure 4.3: One-electron oxidation of pagodanes).

tablished. Within the strained pagodane cages either "tight" or "extended" 4c/3e structures of the pagodane central moieties were located resembling well separated stationary points on the reaction coordinate of the ethylene/ethylene [2+1]cycloaddition (Fig. 4.1). The behavior and persistence of these two types of radical cations is significantly different. Whereas the "extended" isomers were found to be quite persistent in fluid solution even at room temperature, the "tight" species have been detectable only under rather severe conditions, *i.e.*, at low temperature (77 K) in freon matrix or with time-resolved methods. For [1.1.1.1]pagodane, the activation barrier of isomerization from "tight" to extended was determined by fluorescence-detected magnetic resonance (FDMR) at 273 K to be very low (2.2±0.3 kcal mol^{-1})[53], half lifetime 0.15 μs at room temperature. Generally, the "tight" species possess a drastically lower stability than the "extended" ones; whereas generation of "tight" isomer is reversible and back electron transfer could lead to the initial pagodane, the formation of the "extended" radical cations leads either to double bond containing species or to parent radical cation. Therefore, it was not possible to obtain experimental evidence for, especially, "tight" radical cations generated from a number of cage skeletons.

The intriguing feature of CIDNP is that non-equilibrium spin populations caused by the spin sorting are preserved for the relaxation time of the observed nuclei that might be much longer than life time of the radical pair. Thus it could be applied even for observation of very short lived radicals.[54–56]

4.3 Results and discussion

One-electron oxidation of **P1-P7** (0.005 mol l^{-1}) was achieved by irradiation of an equimolar solution of particular pagodane and tetrachloro-1,4-benzoquinone as the electron acceptor at room temperature. The ^{1}H-CIDNP spectra recorded during the above mentioned oxidations are presented on Figures 4.4-4.9. It bocomes evident that the dominating feature of ^{1}H-CIDNP of investigated pagodanes are significant net emissions that can be analyzed by using the Kaptein's rules(see), which are applicable in those cases ($|\Delta g|H_0 > a$). For chloranil, the electron transfer reactions proceed *via* the triplet state;[45] thus $\mu > 0$ and with the g-factor of chloranil radical anion (2.0050)[46] being significantly larger than those of pagodane-type radical cations (*ca.* 2.0031)[47] it follows that $\Delta g < 0$. Since we observe that only NMR transitions of initial pagodanes are polarized (cage recombination, $\varepsilon > 0$) and $\Gamma < 0$ (emission)(Eqn. 2.2):

$$\Gamma_{ne} = \mu \times \varepsilon \times \Delta g \times a$$

$$- = + + - \; a \;\Rightarrow\; a > 0$$

sign of hyperfine coupling constant is positive that is in consent with previous ESR investigations. As the formation of "extended" isomer of radical cation is not reversible during back electron transfer and can rout to starting pagodane molecule all ^{1}H-CIDNP spectra should be attributed to the observation of cyclobutanoid "tight" species.

According to the Radical Pair Mechanism (RPM) theory the polarization is created only when the spin sorting occurs, *i.e.* when both cage and escape products are formed. Therefore there must be two types of polarization present in CIDNP spectra - enhanced emission and enhanced absorption. However in CIDNP spectra of pagodanes only the enhanced emission created by cage products is visible. Also the product analysis shows that no photoproducts different from the parent pagodanes are created. The possible explanation can be done in the following way. The part of "tight" radical cations undergo back electron transfer during the very short time after theirs formation creating net enhanced emission. The second part of also

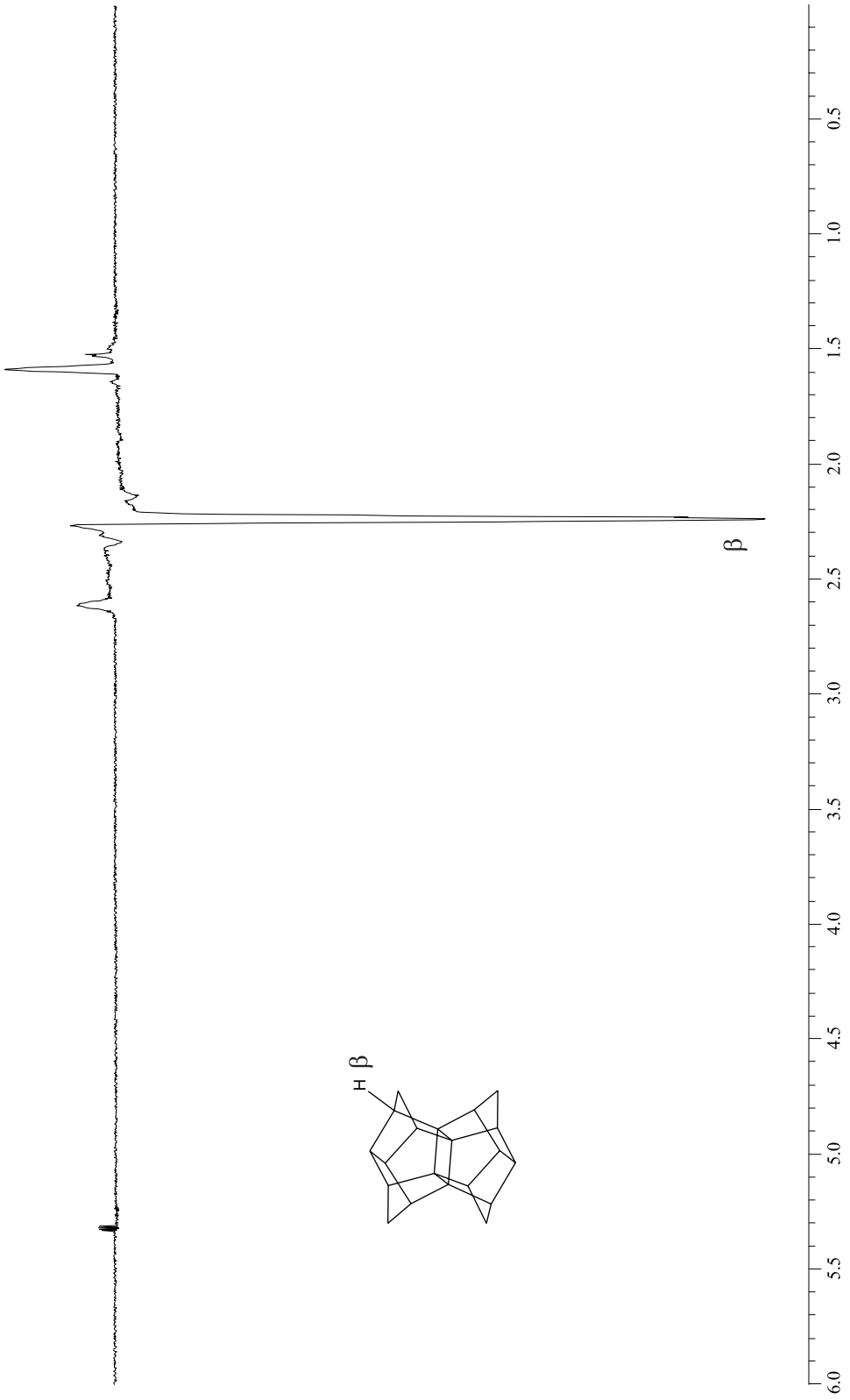

Figure 4.4: ^{1}H-CIDNP spectrum of [1.1.1.1]pagodane **P1**

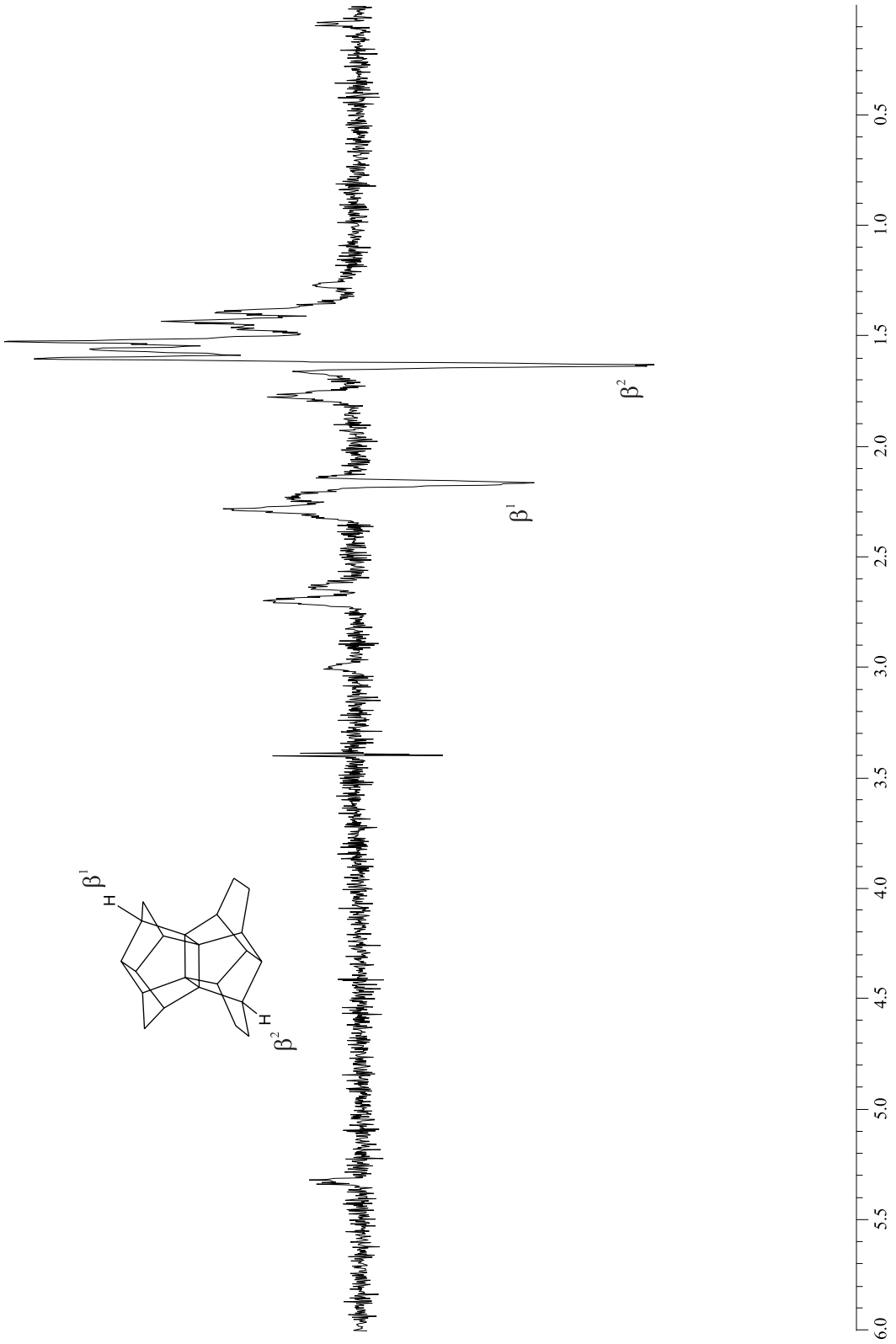

Figure 4.5: ^{1}H-CIDNP spectrum of [2.2.1.1]pagodane **P2**

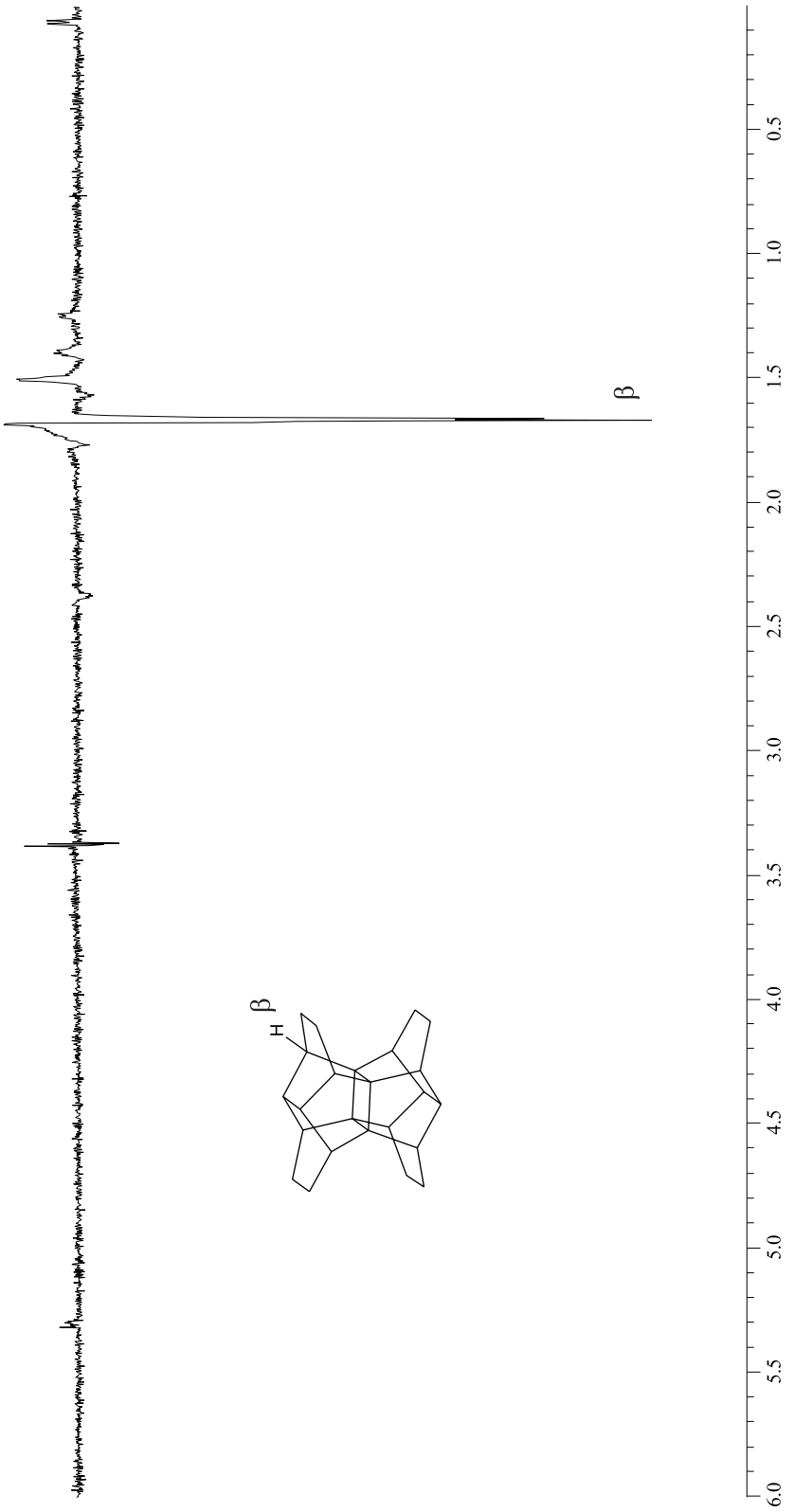

Figure 4.6: ^{1}H-CIDNP spectrum of [2.2.2.2]pagodane **P3**

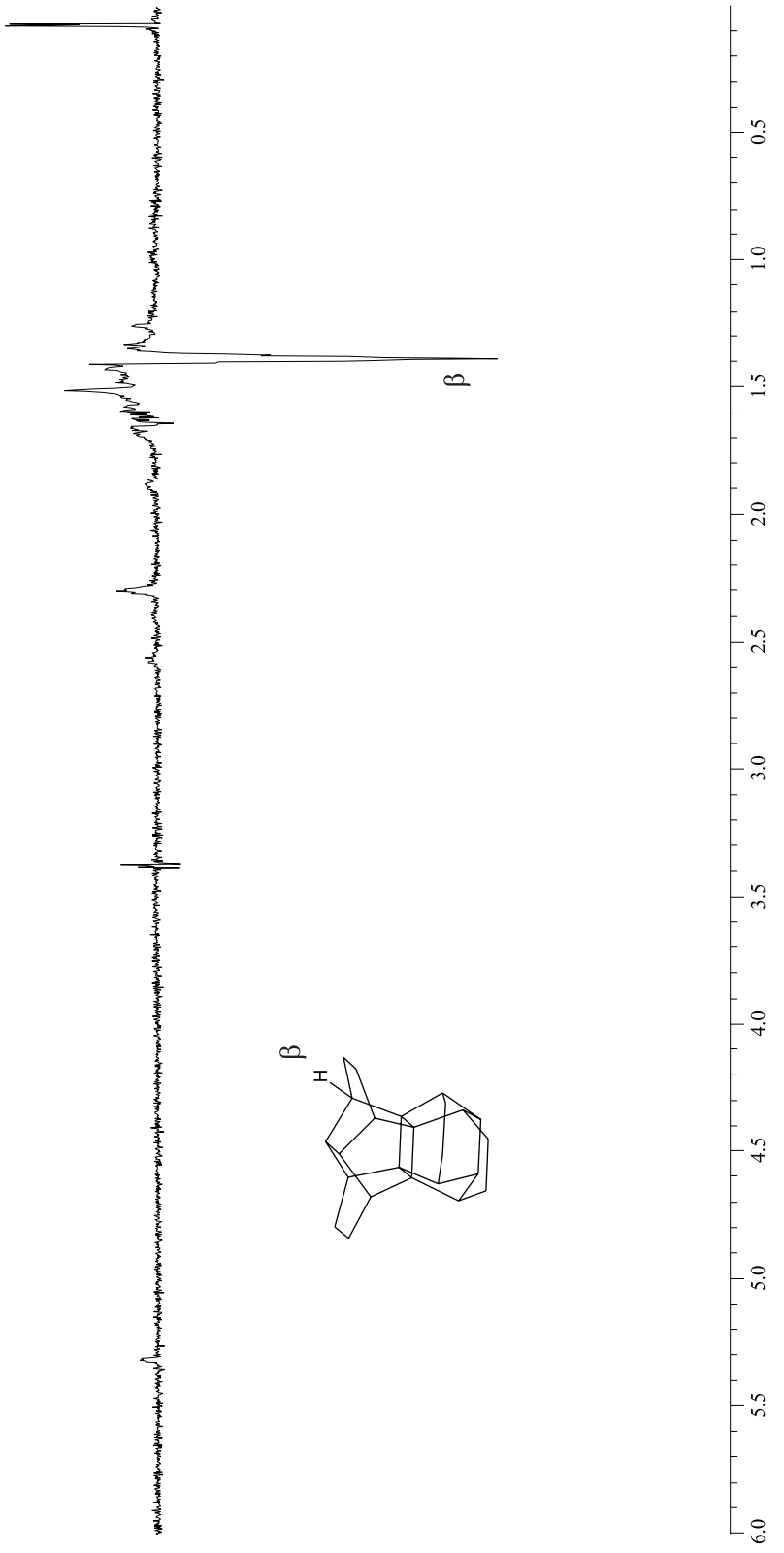

Figure 4.7: ^{1}H-CIDNP spectrum of [2.2.2.2]iso-pagodane **P4**

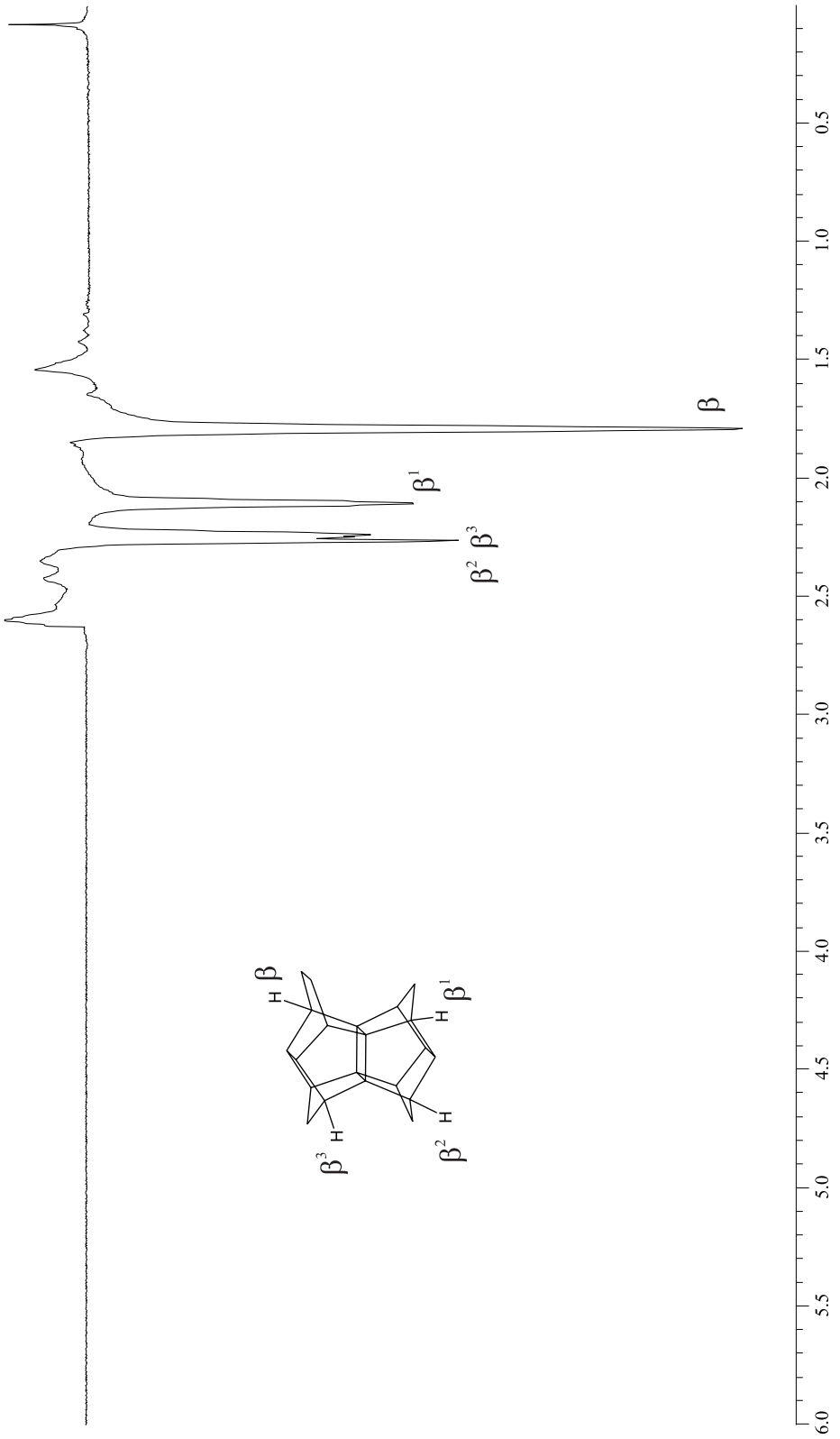

Figure 4.8: ^{1}H-CIDNP spectrum of [2.1.1.1]pagodane **P5**

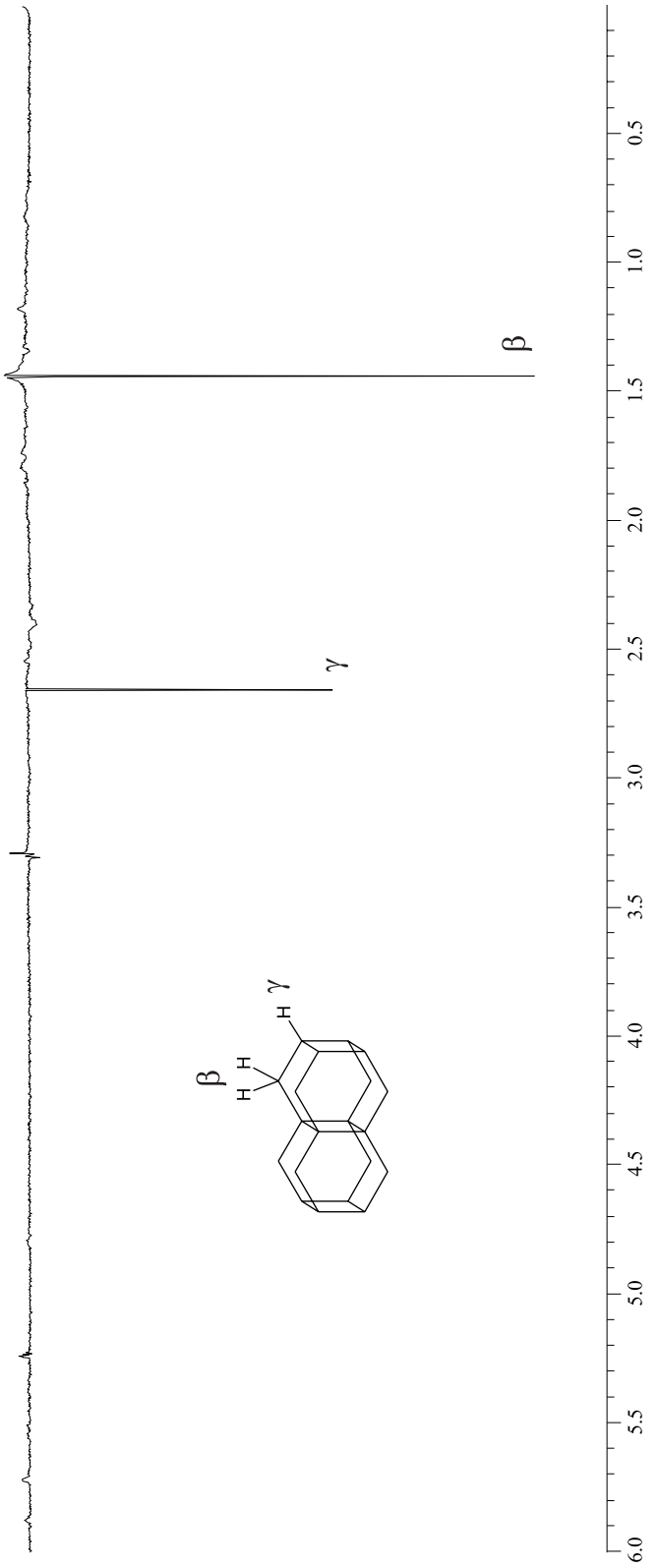

Figure 4.9: ^{1}H-CIDNP spectrum of bis-asteran **P6**

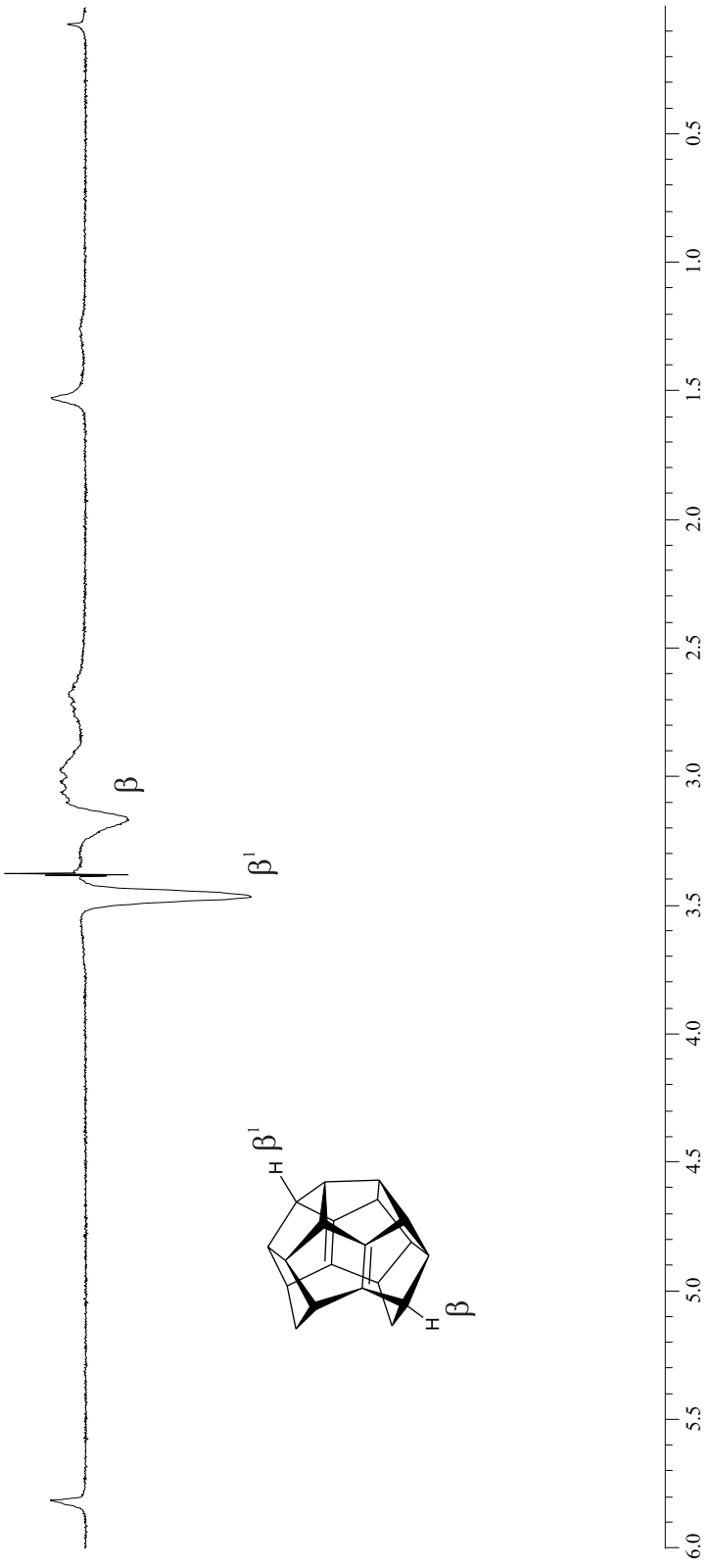

Figure 4.10: ^{1}H-CIDNP spectrum of **P7**

"tight" radical cations stays in the cage for the time which is long enough for the relaxation of the protons. Relaxation drives the spin system to be according the thermal Bolzman distribution. Then they react back producing parent pagodane and no polarization.

Ratios of observed polarizations should represent the ratios between coupling constants of corresponding protons. For some compounds the experimental data on hyperfine coupling constants were not available by ESR. In those cases the results of quantum mechanical calculations have been used. To find both minima ("tight" and "extended") first the structure of parent pagodane was optimized. Then one electron was taken from the optimized structure that led to the geometry of the "tight" isomer. Stretching of two parallel bonds of the central rectangular moiety of the "tight" radical cation with the following optimization produced the geometry for the "extended" species. Both geometry optimization and single point calculations of unpaired electron density were done using B3LYP/6-31G*.

[1.1.1.1]pagodane (P1)

P1$^{\bullet+}$ "tight" radical cation generated from **P1** should possess 8 equivalent β-protons (β with the respect to the central C_4 rectangular moiety of pagodane) with relatively high hfc (1.02 mT by FDMR, 1.05 by UB3LYP 6-31G*)[53] while according to QM calculations hfcs of all other protons must be negligible. Indeed, CIDNP spectrum (Figure 4.4) shows that the only NMR transition polarized is one that corresponds to β-protons (2.24 ppm) of **P1**. "Extended" radical cation must have exhibited rather pronounced couplings of γ-protons.

[2.2.1.1]pagodane (P2)

P2$^{\bullet+}$ possessing two sets of equivalent β-protons exhibits two emissions at 2.15 ppm and 1.61 ppm in CIDNP spectrum(Figure 4.5). The ratio of those two CIDNP polarizations (0.55), which mirrors the ratio of hfcs, is very close to one established by ESR (0.54)[57] and calculations (0.56) for "tight" isomer and differs from calculated for the "extended" one (0.73).

[2.2.2.2]pagodane (P3)

According to QM calculations in $\mathbf{P3}^{\bullet+}$ "tight" and "extended" radical cations - with the C_β-H_β bonds lying almost in the nodal planes orthogonal to the bonds in the SOMO - hyperfine coupling constant of H_β according to calculations should be vanishingly small and can not be used to ascertain the structure of C_4 moiety. It is possible to distinguish between two isomers taking in account γ-γ^2 protons. Whereas in "extended" isomer all γ hyperfine couplings should be very small and

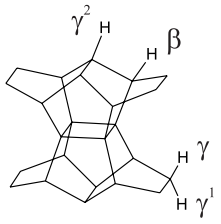

even negative for γ^2 (-0.167 mT), "tight" species must carry quite high spin density on γ^1 (0.627 mT) nuclei and negligible but positive on γ^2. What shows the ^{1}H-CIDNP is: a strong emission at around 1.66 ppm (big positive hfc) and very weak emission at 2.38 ppm (small positive hfc), other NMR transitions of parent **P3** are almost unchanged. All indications point on observation of "tight" isomer.

[2.2.2.2]iso-pagodane (P4)

The radical cation of **P4** was not observed by ESR because of its extreme instability. Application of CIDNP gives a prominent emission at 1.38 ppm and smaller emission at around 1.60. Those transitions correspond to H_β and H_{γ^1} respectively. According to calculations both hydrogen nuclei exhibit rather pronounced hfcs in either "tight" or "extended" radical cations. When in "extended" in radical the hfc of H_{γ^1} is bigger than hfc of H_β, in "tight" the order is opposite, that is in consent with CIDNP measurements.

[2.1.1.1]pagodane (P5)

The D_{2h} symmetry of parent [1.1.1.1]pagodane (**P1**) is not inherited by **P5** thus radical cation carries 4 different sets of equivalent β-protons, that should mirror

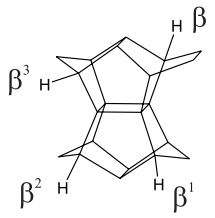

the structure of the central moiety. However in the NMR spectrum it is possible to distinguish only between two of these sets: β (1.78 ppm) and β^1 (2.01 ppm). Ratio of corresponding CIDNP polarizations (2.36) better fits to "tight" structure (hfc_β/hfc_{β^1}=2.15) rather than to "extended" one (hfc_β/hfc_{β^1}=0.87).

bis-asteran (P6)

The D_{4h} symmetry of **P6** should be retained in "tight" radical cation, which consequently must possess 16 equivalent β-protons and 8 γ ones. In the "extended" radical symmetry is changed to D_{2h} with two magnetically different proton sets (8 protons in each set) of different type and therefore exhibiting different hfcs. The equivalence of γ-protons is preserved. If we assume that "extended" species can react back to produce **P6**, the CIDNP polarization appearing from β-protons must be an average estimate of both coupling constants. QM examination of "tight" and "extended" bis-asteran radical cations shows the following β and γ hyperfine coupling constants: "tight" - $hfc_\beta = 0.98$ mT, $hfc_\gamma = 0.5$ mT, "extended" - $hfc_\beta = 1.95$ mT, $hfc_{\beta^1} = -0.08$ mT, $hfc_\gamma = 0.73$ mT. Taking into account the polarization averaging of β and β^1 that would have been occurred with "extended" radical cation, the ratio of polarizations of two NMR transitions is 1.28 ($[hfc_\beta+hfc_{\beta^1}]/hfc_\gamma$). For "tight" it is 1.96. Experimental results produce ratio of polarizations equal to 2.3 which is more close to parameters of "tight" radicals.

pagodadiene (P7)

In contrast to pagodanes and bis-asteran, pagodadiene **P7** does not contain the C_4 rigid moiety and its radical cation does form any of two isomers characteristic to pagodane radical monocations. Nevertheless one electron transfer from the **P7** leads to the species that are observed by CIDNP and even ESR. Detection of $\mathbf{P7}^{\bullet+}$ by

ESR points on its higher persistence compared to "tight" isomers of pagodane radical cations. That is also in consent with the line broadening of the CIDNP polarizations. That broadening tells that the lifetime of the radical pairs is comparable with the relaxation times of observed protons in the paramagnetic species which lies in the range $10^{-4} - 10^{-3}$s. The ratio of polarizations of two sets of β-protons is 0.76 which is rather different from the calculated value 0.98. The difference between the measured and the calculated values probably arises because of the ion pairing and short relaxation times of the observed nuclei.

Although qualitative treatment gives definitive description of the radical cations structures, it would be very intriguing to use CIDNP spectra of pagodanes for the calculation of absolute values of hyperfine coupling constants. If we assume that

- hyperfine coupling constants are in range -20 mT - 20 mT
- all radical cations have similar magnetic properties, which is true (g-factors are almost identical)
- quantum yields of the oxidation reactions of pagodanes are similar (redox potentials of pagodanes are comparable)
- observed protons are not coupled to any other protons *i.e* observed protons represent the A spin system, what is true because the dihedral angles between observed protons are close to 90° that according to Karplus rule will lead to very small spin-spin coupling
- diffusion properties of radicals are similar

that will make allow us to use the equation 2.12 (section 1.3) and follow up linear dependence 2.13 to calculate hfcs of examined radical cations. The proportionality constant C is the same for all studied systems since experimental conditions are the same (*i.e.* concentration of pagodanes and chloranil, temperature, light intensity are constant) and we use above mentioned assumptions. The constant C itself was calculated using very well established by ESR hyperfine constants of "tight" radical

cation of [2.2.1.1]pagodane (C=[I T]/hfc) and equals 0.00762 Wb m^{-3} s^{-1}.[a] β and γ hyperfine coupling constants evaluated using the obtained constant C are collected in tables 4.1 and 4.2 respectively.

Table 4.1: Experimental and theoretical ^{1}H hfc assigned to the β-protons of the pagodane type radical cations

	^{1}H-hfcs(β-protons)/mT			
Radical cation	Experimental		Calculated UB3LYP/6-31G*	
	ESR	CIDNP	"tight"	"extended"
[1.1.1.1]pagodane **P1**	1.544	1.04	1.01	1.48
[2.2.1.1]pagodane **P2**	0.96/1.76	0.96/1.76	1.73/0.97	1.11/1.54
[2.2.2.2]pagodane **P3**	0.06	very small	−0.03	0.001
[2.2.2.2]iso-pagodane **P4**	N/A	1.02	1.64	1.13
[2.1.1.1]pagodane **P5**	N/A	0.89/2.1	2.46/1.14	1.38/1.59
bis-asteran **P6**	N/A	1.21	0.98	−0.08/1.95
P7	N/A	1.18/1.55	1.49/1.52	

It is obvious that values obtained by ^{1}H-CIDNP are in very good agreement with both ESR and calculated with density functional theory. Moreover, quantitative CIDNP measurements better fit to the theoretically obtained for "tight" radical cations that is in consent with the reversibility of pagodanes oxidation and qualitative analysis of CIDNP polarizations.

[a] the dimensions of C are calculated taking in account that CIDNP polarization I is dimensionless value

Table 4.2: Experimental and theoretical ^{1}H hfc assigned to the γ-protons of the pagodane type radical cations

	^{1}H-hfcs(γ-protons)/mT			
Radical cation	Experimental		Calculated UB3LYP/6-31G*	
	ESR	CIDNP	"tight"	"extended"
[2.2.2.2]pagodane **P3**	0.58	0.61	0.63	0.16
[2.2.2.2]iso-pagodane **P4**	N/A	0.30	N/A	1.63
bis-asteran **P6**	N/A	0.52	0.5	0.73

4.4 Conclusions

Were detected radical cations, which were not available within the direct ESR and cyclovoltametric methods. A very simple method for calculation of hyperfine coupling constants using dynamic nuclear spin polarization is in excellent agreement with both ESR experimental and theoretical data. According to quantum mechanical calculations the reversibility of the radical cation formation is the first indication for the observation of the "tight" radicals, since only this stage is reversible. That is also supported by qualitative and quantitative analysis of CIDNP spectra.

Chapter 5

Quantitative ^{31}P-CIDNP and NMR of mono- and bisacylphosphine oxides

The liquid mixture of monomers or/and oligomers can be converted to a solid polymer by radical polymerization reaction. If it is required to perform that process under the light irradiation the component called photoinitiator must be used in most cases. The photoinitiator absorbs a light energy and converts it into chemical one and initiates polymerization. The initiating free radicals can be generated *via* either homolytic bond scission or be electron transfer reaction.

To be efficiently used as the commercial product in the industrial applications the radical photoinitiator must fulfill certain requirements:

- absorb light at the desired wavelength
- produce the radicals with the high efficiency
- the produced radicals must be reactive towards the monomer/oligomer
- the radicals should not be sensitive to oxygen which is usually present

- the photoproducts should not absorb in the visible range and should not mask the absorption of the photoinitiator itself

The overall performance of photoinitiator will be determined by the combination of those factors. Also the monomer itself plays an important role being responsible for the so called growing chain effects.

Among the above mentioned requirements the reactivity of the initiating radicals to the monomer seams to be the most important since it does determine how fast and efficient the polymerization is initiated. The reactivity towards monomer also influences the waste reaction with oxygen.

The following study presents the systematic investigation of electronic properties of phosphinoyl radicals by QM calculations, NMR and their relation to CIDNP effects and first addition to the monomer.

5.1 Compounds investigated

Monoacylphosphine oxides (MAPO) and bisacylphosphine oxides (BAPO) have

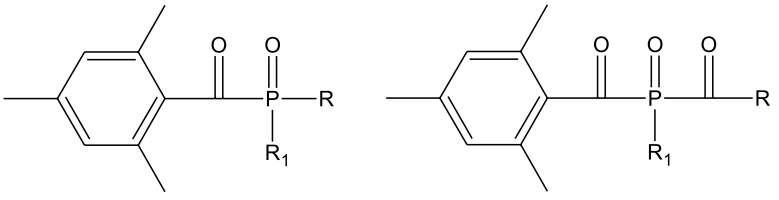

monoacylphosphine oxide

bisacylphosphine oxide

been introduced quite recently[58] as a very efficient photoinitiators for photoinduced polymerization. Those compounds possess number of very intriguing features that provide efficient initiation of polymerization. Under light excitation MAPOs and BAPOs undergo α-cleavage (Figure 5.1) producing a benzoyl and phosphinoyl radical pair which in turn undertakes singlet-triplet mixing. The rate and efficiency

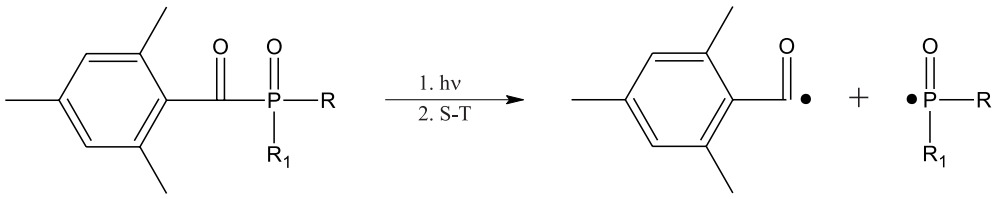

Figure 5.1: α-cleavage of mono- and bisacylphosphine oxides

of that mixing and therefore the reaction probability for the radical pair is directly dependent on the hyperfine coupling constant of participating radicals. Very high coupling constant of ^{31}P nuclei in phosphinoyl radicals (20-80 mT) compared to most carbon centered radical (1-3 mT) gives phosphorus-centered radicals an obvious advantage in singlet-triplet mixing. Another important property of phosphinoyl radical is exceedingly high reactivity towards carbon-carbon double bonds. That reactivity is normally few orders of magnitude higher than addition to carbon-centered initiating species. All that makes phosphinoyl based photoinitiators highly attractive for use in various polymerization applications.

The structures of mono- and bisacylphosphine oxides investigated are collected on figures 5.2, 5.3 and 5.4 correspondingly. The **R** represents on those figures 2,4,6-trimethylbenzoyl substituent:

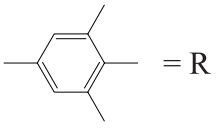

5.2 Absorption spectra

The absorption properties of mono- and bisacylphosphine oxides are similar but differ from the characteristics of other photoinitiators α-cleavage type (α-amino ketones, α-hydroxy ketones, α-oxooximes). They possess quite high absorption in the

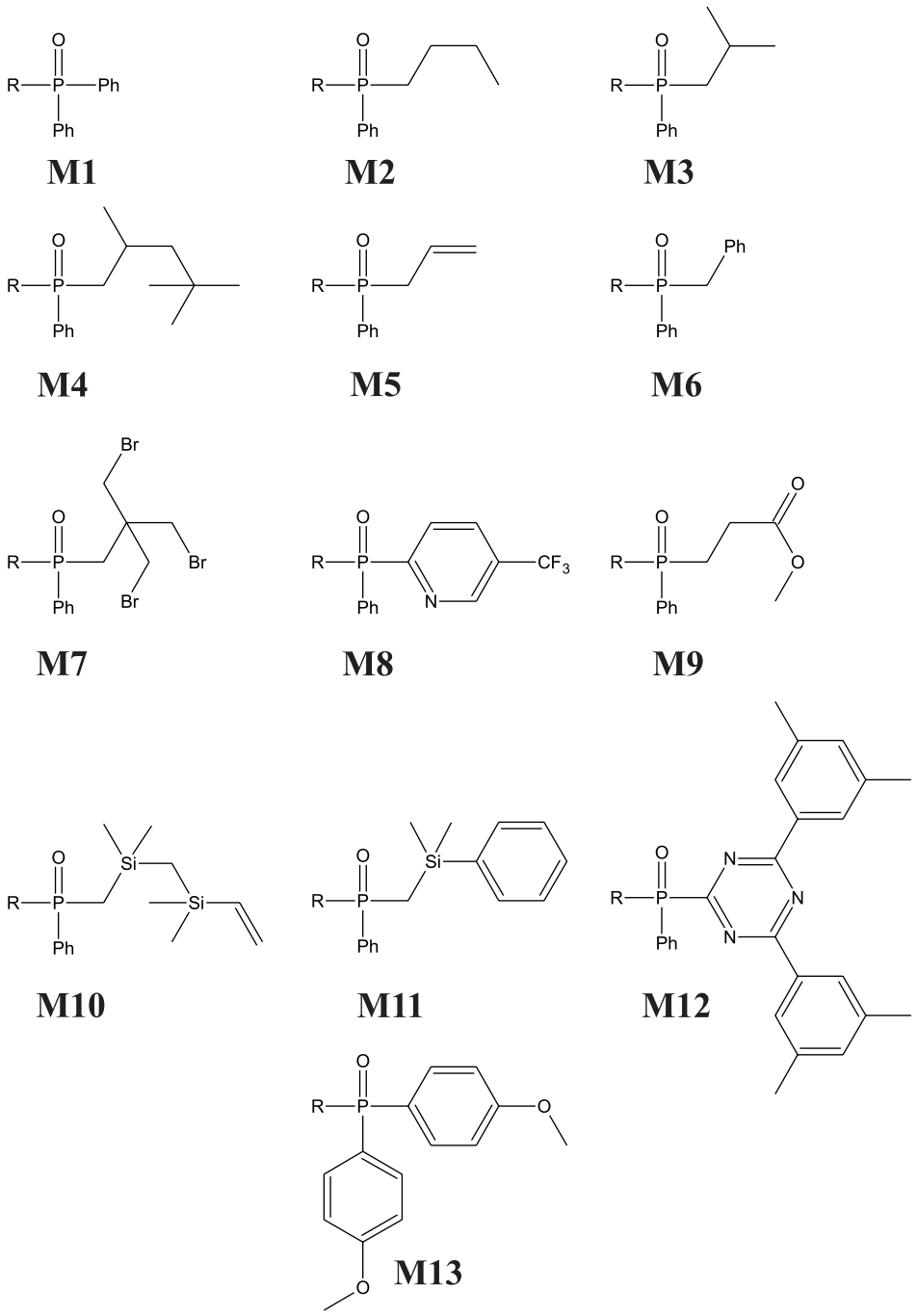

Figure 5.2: MAPOs investigated

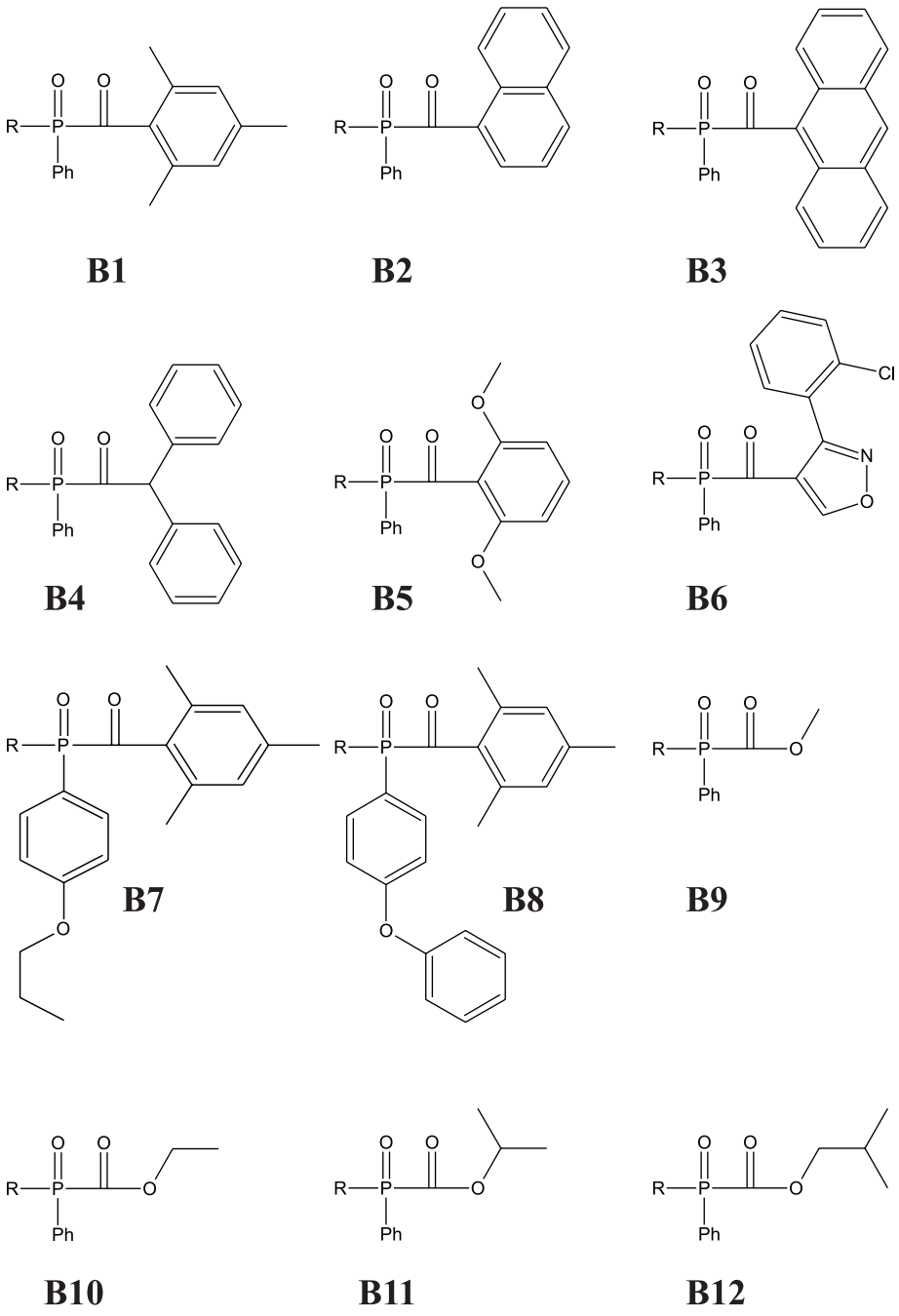

Figure 5.3: BAPOs investigated

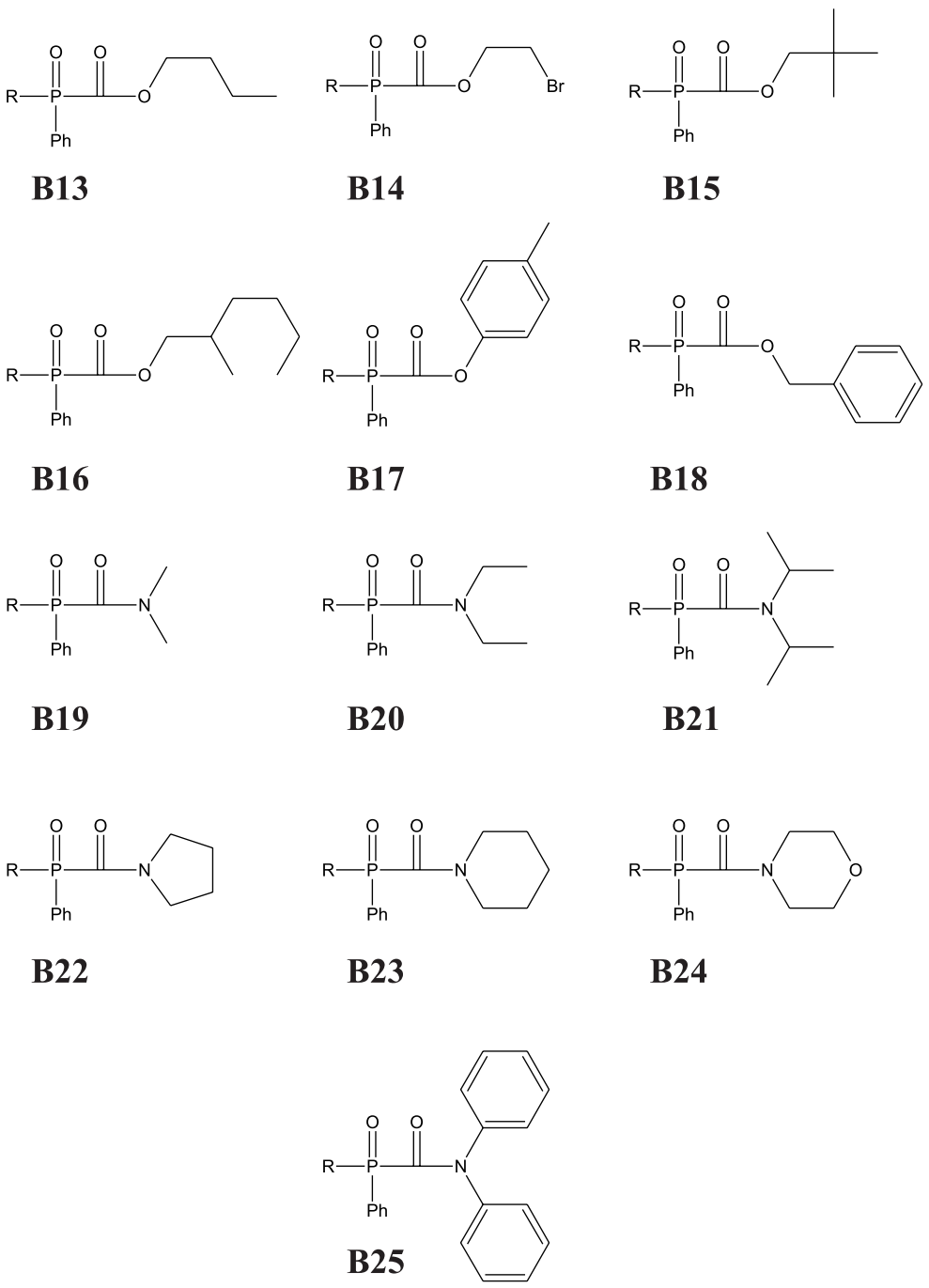

Figure 5.4: BAPOs investigated

near UV and visible range The ground state absorption spectra of these substances have absorption maximum at about 300 nm and 385 nm. the absorption bands with the highest intensities were assigned to the $\pi \rightarrow \pi^*$ electronic transition whereas bands with the lower intensities have been identified as the $n \rightarrow \pi^*$ transitions. Absorption spectra of some selected MAPOs and BAPOs are shown on Figures 5.5

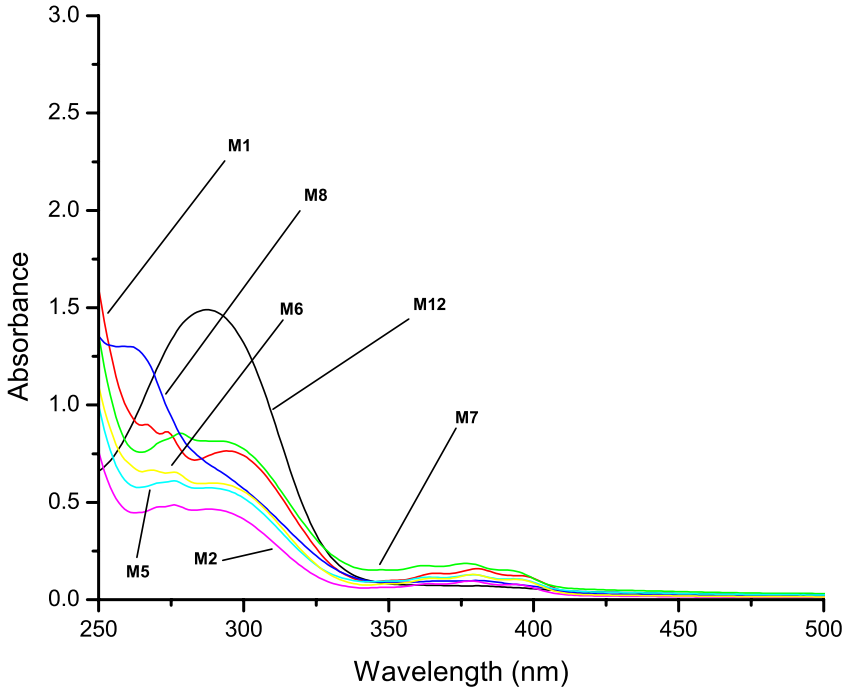

Figure 5.5: Absorption spectra of selected MAPOs

and 5.6 correspondingly. The batochromic shift of the low-energy absorption bands of BAPOs compared with the corresponding electronic transitions of MAPOs is presumably due to the extension of the electronic conjugation to the second carbonyl group. It is clear that most of bisacylphosphine oxides absorb light at wavelengths above 380 nm more efficiently than MAPOs. This will apparently lead to the higher initiation performance in, for example, wight pigmented systems where rutile-type titanium dioxide is used as a pigment and acts as a very effective screen for the light

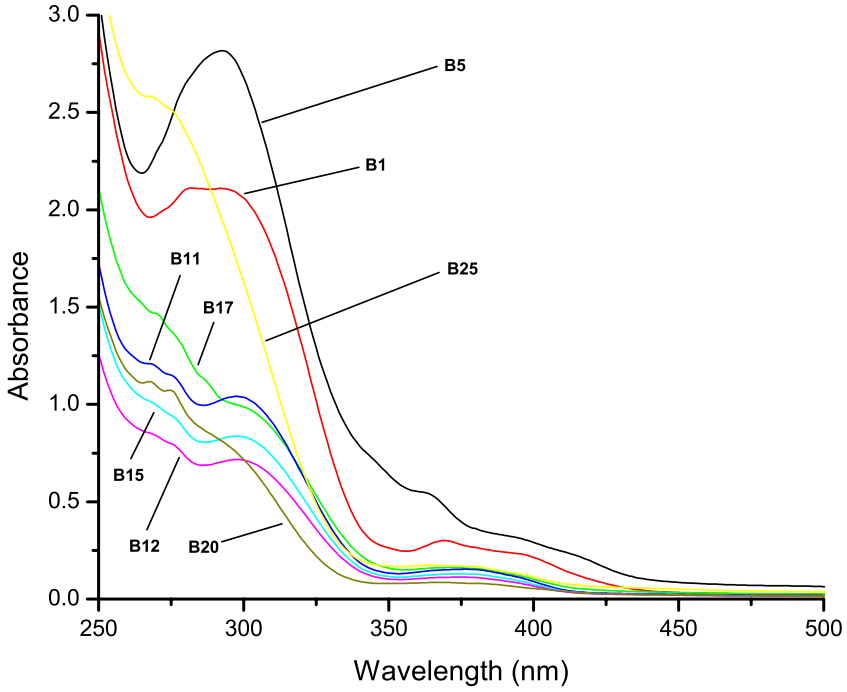

Figure 5.6: Absorption spectra of selected BAPOs

of all wavelengths below 380 nm.

Another important feature of most MAPOs and BAPOs is photo-bleaching. The chromophore of those phosphine oxides that absorbs energy in the visible and near UV range is destroyed upon light irradiation and subsequent bond cleavage - resulting photoproducts are transparent. That is extremely useful in cure of high thickness films and surfaces since there is no masking by photoproducts and yellowing occur.

Molar extinction coefficients at wavelengths 308 nm (ε_{308}) and 342 nm (ε_{342}) which were used for the irradiation in the present study are collected in Table 5.1.

Table 5.1: Molar extinction coefficients at 308 nm and 342 nm of compounds investigated

Compound	$\varepsilon_{308}(\mathrm{mol^{-1}cm^{-1}})$	$\varepsilon_{342}(\mathrm{mol^{-1}cm^{-1}})$
M1	1890	279
M2	973	179
M3	1373	200
M4	1900	318
M5	6300	230
M6	1368	230
M7	1972	462
M8	1400	297
M9	6230	240
M10	5280	290
M11	1169	199
M12	3097	1300
M13	2100	270
B1	5606	994
B2	6107	6344
B3	5516	3833
B4	4446	329
B5	6939	2269
B6	2185	348
B7	3400	480
B8	3580	520
B9	3025	470
B10	2676	482
B11	2833	508
B12	1964	518
B13	2588	463

Table 5.1: *continued*

Compound	$\varepsilon_{308}(\mathrm{mol^{-1}cm^{-1}})$	$\varepsilon_{342}(\mathrm{mol^{-1}cm^{-1}})$
B14	2028	444
B15	2289	390
B16	2407	437
B17	2723	622
B18	2996	572
B19	2488	399
B20	1709	257
B21	1988	257
B22	2052	306
B23	2109	293
B24	1527	327
B25	3742	567

5.3 Previous studies

Since mono- and bisacylphosphine oxides are being extensively used in industry for various photopolymerization applications, they have been investigated with diverse methods at different conditions. Particular attention has been payed to parent 2,4,6-trimethylbenzoyldiphenylphosphine oxide **M1** and bis-(2,4,6-trimethylbenzoyl)-phenylphosphine oxide **B1**.

By the use of time-resolved chemically induced dynamic electron polarization spectroscopy (TR-CIDEP) 2,4,6-trimethylbenzoylphosphine oxide **B1** has been found to undergo α-cleavage from the triplet state.[59, 60] The ESR spectra of both phosphinoyl and benzoyl radicals were recorded. The structure of radicals produced via α-cleavage has been confirmed by radical trapping experiments. Both the substituted phosphinoyl and benzoyl radicals were found to be reactive towards electron-rich double bonds in acrylates, styrenes and related double bond contain-

ing monomers[61–64], has been deduced that the phosphinoyl radical is more than two times as effective as the benzoyl in polymerization initiation. FT-IR and UV studies were done by the use of acylphosphine oxides as initiators for curing of acrylate and unsaturated polyester resins[65, 66]. It was found that the efficiency of photoinitiation by acylphosphine oxides is very sensitive to oxygen *i.e* dramatically reduced in its presence, though TR-ESR investigations claim that addition of phosphinoyl radicals to oxygen is slower than of benzoyl one which serves as the oxygen quencher[67]. The comprehensive investigations on reaction mechanism of mono- and bisacylphosphine oxides were performed by ^{31}P-, ^{1}H-, ^{13}C-CIDNP and ESR, the complete pathways of photoreactions of phosphine oxides have been evaluated.[68]. Numerous experimental methods have been applied for the determination of the absolute rate constants of the addition of phosphinoyl radicals to diverse monomers. At room temperature the addition constant of those radicals lie in the range $10^6 - 10^7$ $M^{-1}s^{-1}$.[69–74] The hypothesis made on the basis of quantum mechanical calculations and experimental data on addition constants claims that the rate of the addition of phosphinoyl radical to a double bond containing monomer strongly depends on the extend of the pyramidalization of phosphorus atom in those paramagnetic species.[75] In other words, the rate of the addition increases with the increase of the s-character of the unpaired electron that is mostly localized on the phosphorus. Although experimental data on first addition are in rather good agreement with theoretical calculations it is important to notice that all above mentioned quantitative investigations were done in the conditions that are quite far from real industrial applications (high viscosity, very big excess of monomer, presence of oxygen). In those conditions phosphinoyl photoinitiators were found to increase their initiating efficiency under the application of moderate magnetic field.[76]

5.4 ^{31}P-CIDNP of acylphosphine oxides

The first step in the photodegradation of mono- and bisacylphosphine oxides is the formation of primary spin-correlated radical pair, which consists from phosphinoyl and benzoyl radicals, via the α-cleavage of C(O)-P bond that follows intersystem

crossing. An electron spin density distribution on phosphinoyl radical is adequately

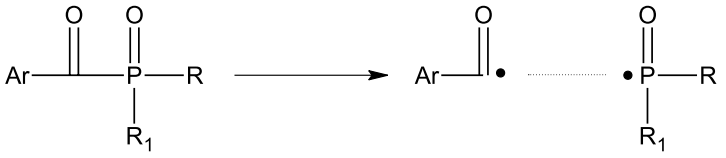

described by the superposition of two canonic structures where the unpaired electron is located either on phosphorus or on oxygen atom.

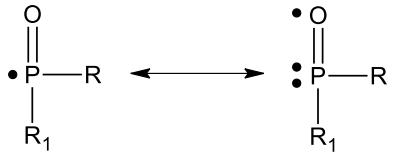

The primary radicals formed during photolytical α-cleavage of carbon-phosphorus bond may form two different types of products: cage and escape. The cage type of products (cage products) is formed by reencounter of primary radicals after some diffusive excursion, whereupon they do either recombine or disproportionate. Figure 5.7 shows the possible recombination reactions of the primary radical pair of 2,4,6-trimethylbenzoylphosphine oxide **M1**. Recombination and disproportionation cage reactions correspondingly lead to formation of the initial phosphine oxide **M1** and disproportionation product **M1-1** which is relatively unstable and is oxidized in a few seconds to give **M1-2**. Oxidation of **M1-1** is particularly fast in the presence of water and oxygen.

The escape products appear when after α-cleavage and certain diffusion steps phosphinoyl and benzoyl radicals may leave the cage and reencounter other radicals. The structures of primary radicals suggest four possible products of escape reactions. One due to recombination of benzoyl radicals and three escape products of phosphinoyl radicals. The possible escape reaction pathways are shown on Figure 5.8.

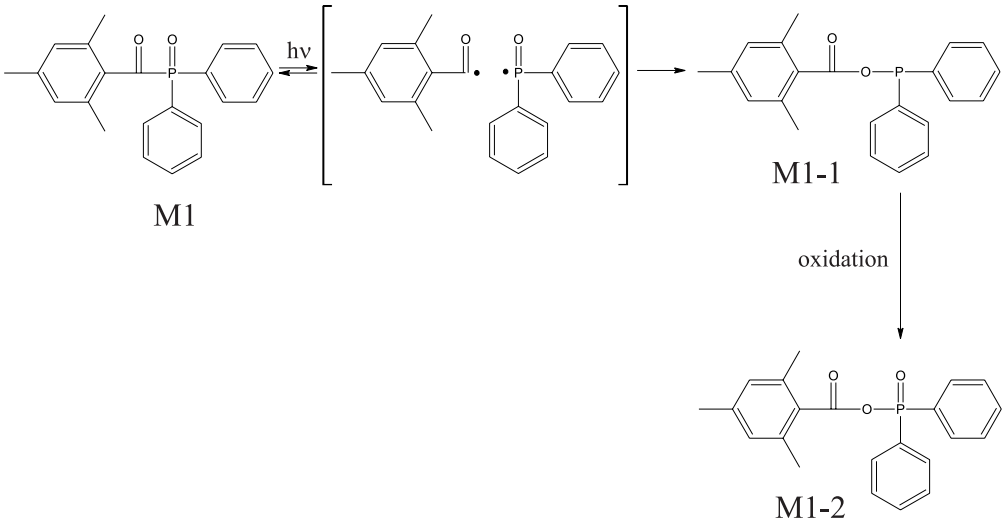

Figure 5.7: Possible cage reactions of **M1**

Both escape and cage products give rise to the polarization in CIDNP experiments(except for **M1-2** since it is not formed via radical coupling). Polarization pattern (enhanced emission/absorption) gives an information on the type of product (cage/escape), difference between g-factors and sign of the phosphorus-phosphorus coupling constant (hfc) in **M1-5**. Intensity of polarization retains "knowledge" on the value of hfc, concentration and diffusion properties of radicals that reacted forming diamagnetic products. Figure 5.9 presents ^{31}P-CIDNP spectrum of **M1** at relatively high concentration of the substance (0.05 mol/l) where signals of almost all products that possess phosphorus nuclei (**M1, M1-1, M1-4, M1-5**) are polarized. The third possible escape product containing P-O-O-P fragment (**M1-6**) is not detected, which is not surprising from the point of view of the expected stability. It possibly rapidly rearranges to **M1-5**.

However ^{31}P-CIDNP spectra taken at a lower concentration (0.015 mol/l) of **M1** retain only few of the features of spectra obtained at a higher one. The signal corresponding to **M1-5** is not present anymore while formation of the escape product **M1-4** and especially two cage recombination species **M1**, **M1-1** is still quite pronounced (Figure 5.10). Indeed, product analysis by ^{31}P-NMR spectroscopy in-

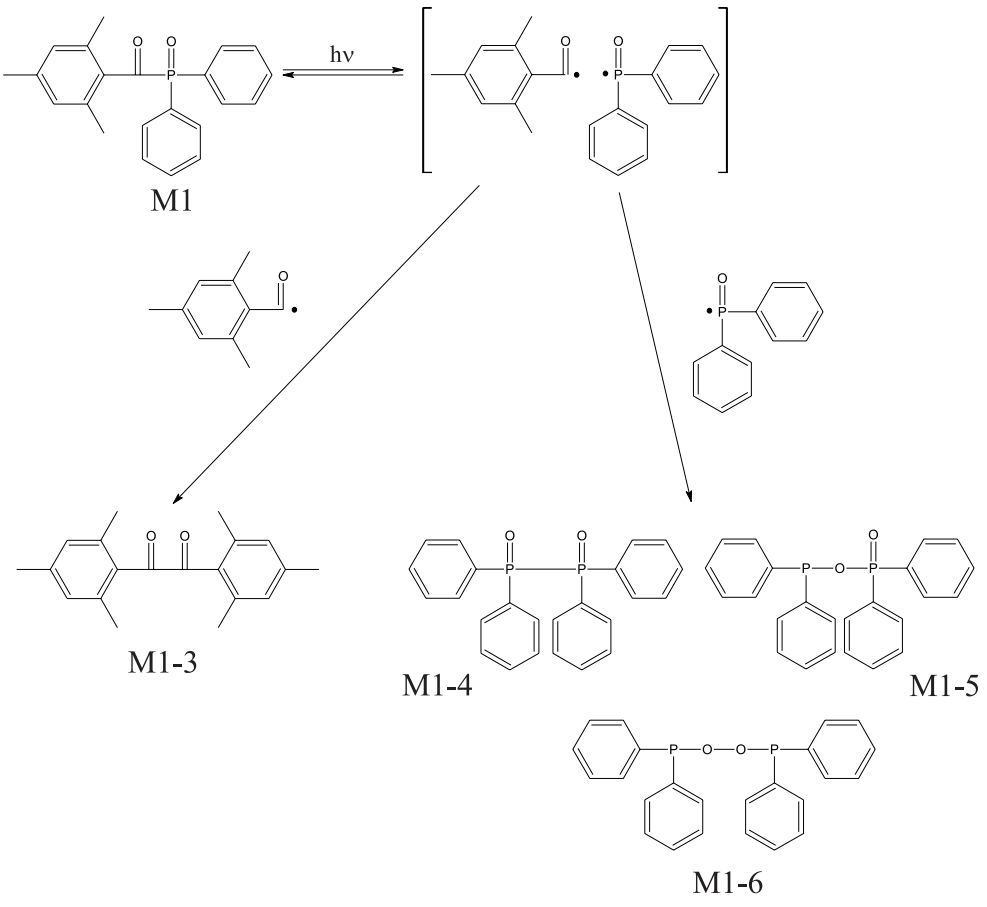

Figure 5.8: Possible escape reactions of **M1**

dicates, in addition to the initial **M1**, domination of **M1-1** and **M1-4**. Strictly speaking, **M1-1** was not found in the relaxed NMR spectra due to its extreme instability and sensitivity versus water. The conclusion has been done on the basis of observation of the products of hydrolysis and oxidation of **M1-1**.

The photochemical behavior of bisacylphosphine oxides is pretty the same as of monoacylphosphine oxides. After homolytical cleavage of C(O)-P(O) bond two possible cage and three escape products could be formed by the reaction of free radicals. Four of the products carry the phosphorus nuclei and therefore appear in ^{31}P-CIDNP spectrum. The only exception occurs when bisacylphosphine oxide has

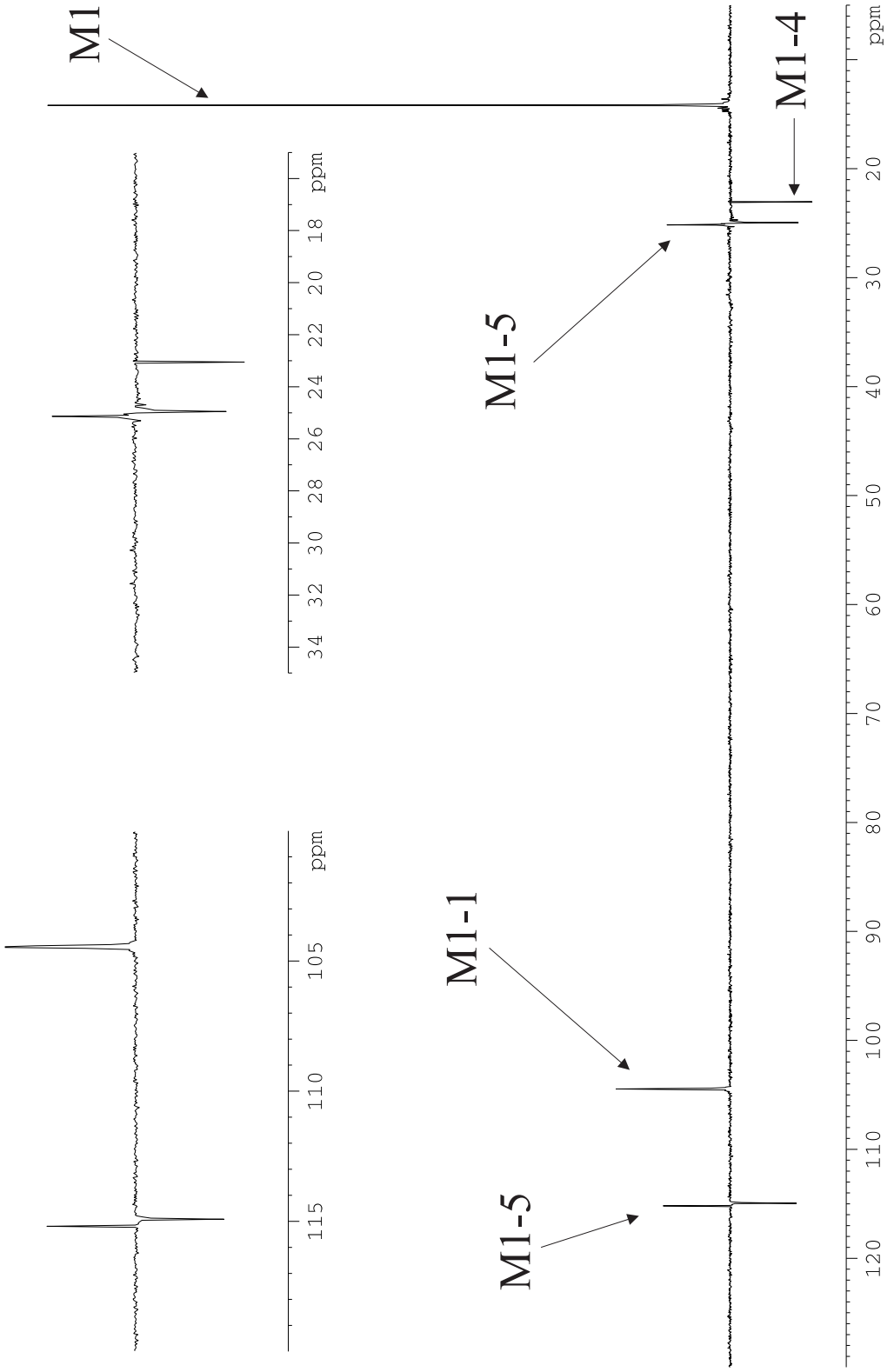

Figure 5.9: ^{31}P-CIDNP spectrum of **M1**(0.05 mol/l, 342.5 nm, benzene-d6)

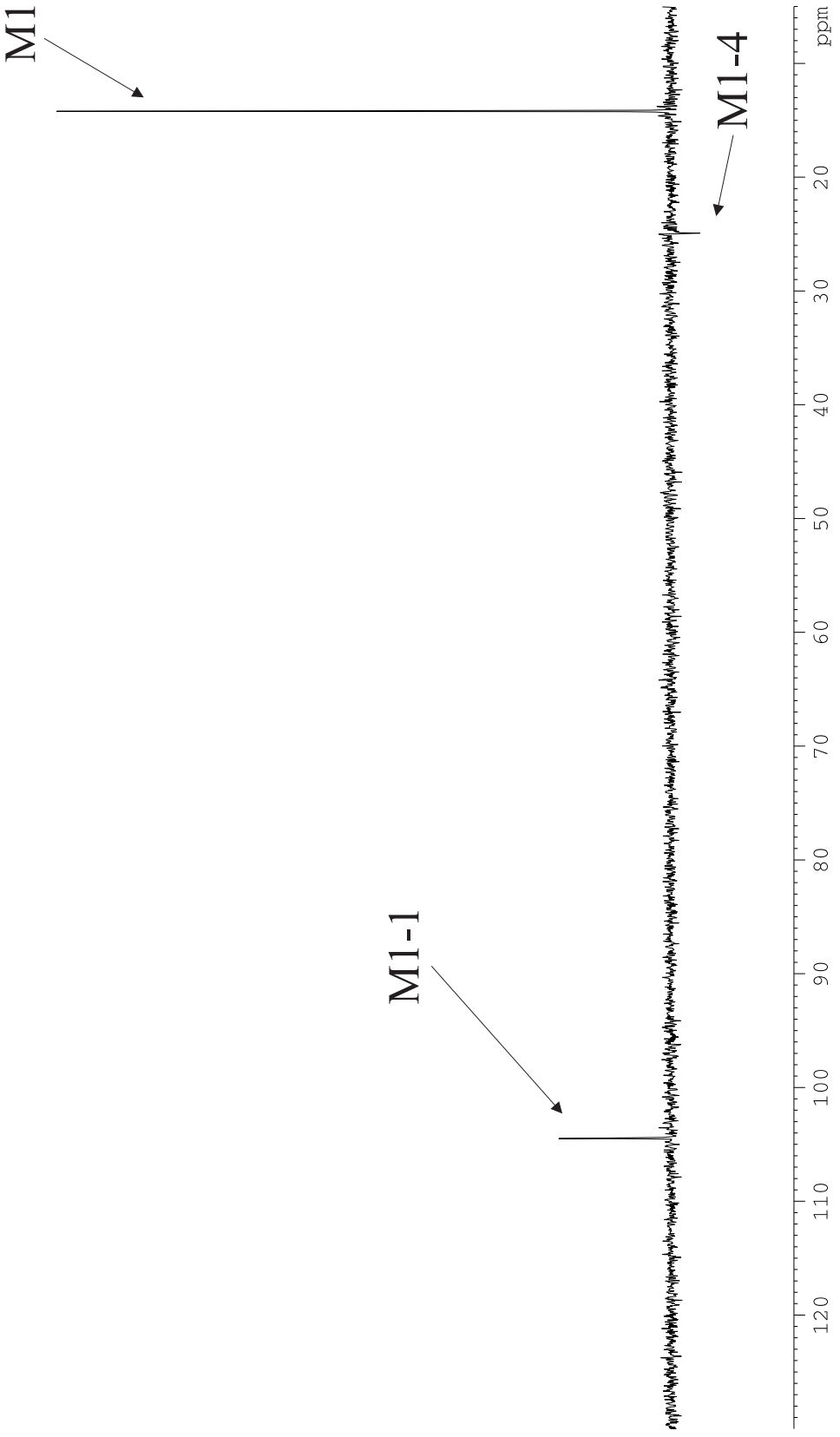

Figure 5.10: ^{31}P-CIDNP spectrum of **M1**(0.025 mol/l, 342.5 nm, benzene-d6)

a possibility to be cleaved at the second C(O)-P(O) bond in that case the reaction pattern looks more complicated because of the increased number of possible cage and escape products.

The concentration dependence of ^{31}P-CIDNP spectra of BAPOs remains the same as of MAPOs. Only three reaction with participation of radicals are visible in ^{31}P-CIDNP experiments at low concentrations, the formation of the second escape product containing P-O-O-P) fragment is negligible. The sample ^{31}P-CIDNP spectra of **B10** is shown on Figure 5.11. It is obvious that the polarizations of both cage products are dominating. Also the ^{31}P-NMR product analysis is in consent with the CIDNP observations.

5.5 Results

5.5.1 ^{31}P-CIDNP

NMR (and CIDNP) transitions of two cage products, recombination and disproportionation, containing phosphorus nuclei in different oxidation states (**V**) and (**III**) correspondingly are dominating in the ^{31}P-CIDNP spectra of MAPOs and BAPOs possessing very high CIDNP polarizations and therefore are easy to measure. Chemical shifts of those CIDNP transitions of MAPOs and BAPOs that do not overlap are collected in tables 5.2 and 5.3 respectively.

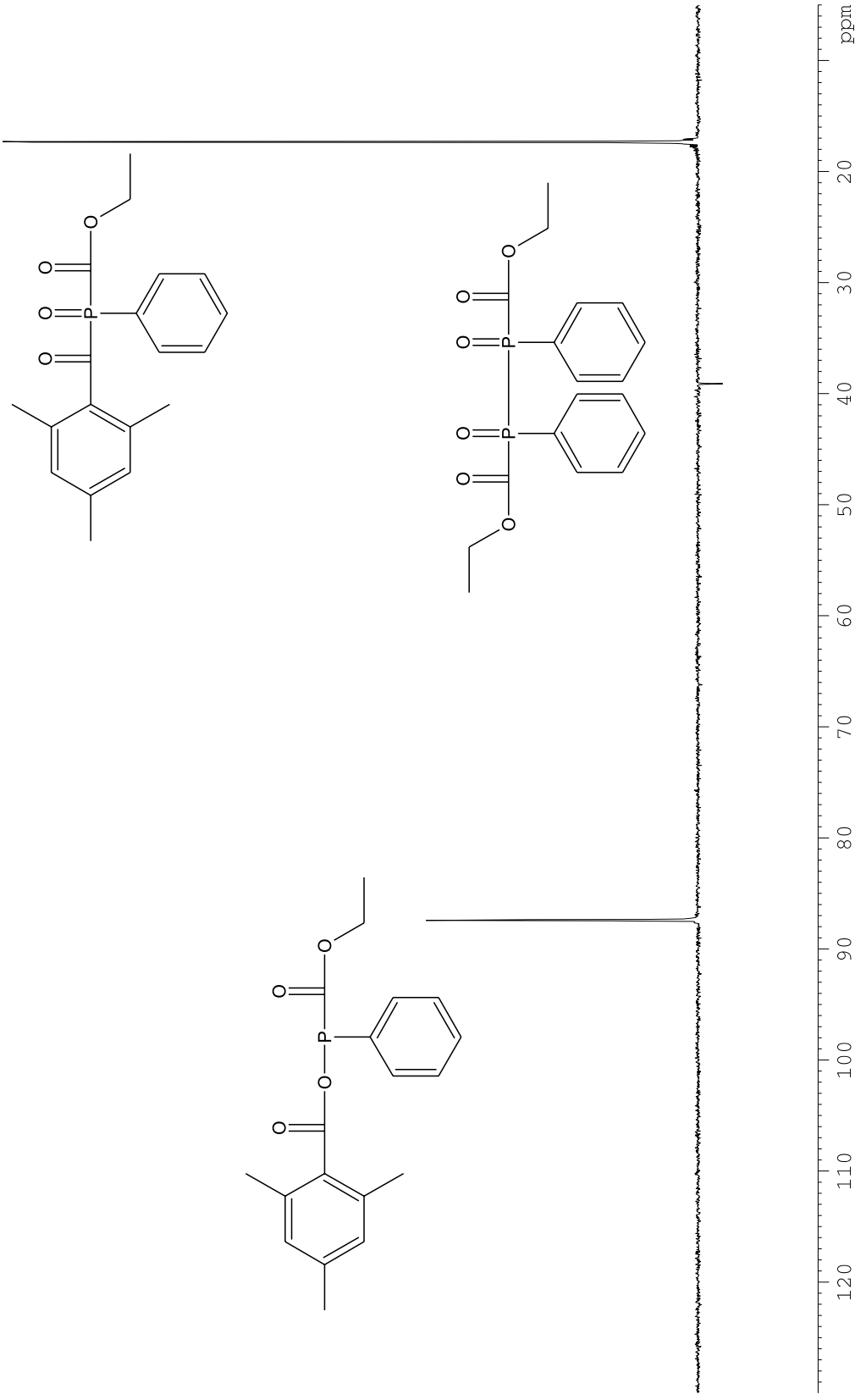

Figure 5.11: ^{31}P-CIDNP data of **B10**(0.025 mol/l, 342.5 nm, benzene-d6)

Table 5.2: Chemical shifts and longitudinal relaxation times of the phosphorus nuclei in cage products of MAPOs photoreactions

Compound	Chemical shift of P(III)(ppm)	Chemical shift of P(V)(ppm)	Longitudinal relaxation time of P(V)(T_1,s)
M1	104.69	14.18	7.33
M2	111.72	27.61	6.09
M3	98.78	7.92	6.02
M4	115.93	29.82	7.65
M5	97.85	8.15	7.39
M6	93.55	10.32	3.98
M7	117.04	31.24	7.54
M8	109.46	24.49	4.42
M9	105.92	19.85	7.12
M10	101.22	11.79	4.31
M11	82.87	16.40	7.12
M12	91.90	12.05	8.88
M13	99.30	14.63	8.1

Table 5.3: Chemical shifts and longitudinal relaxation times of the phosphorus nuclei in cage products of BAPOs photoreactions

Compound	Chemical shift of P(III)(ppm)	Chemical shift of P(V)(ppm)	Longitudinal relaxation time of P(V)(T_1,s)
B1	87.34	10.66	6.56
B1	97.50	10.55	7.34
B3	102.06	13.47	6.24
B4	102.68	12.67	5.57
B5	107.03	20.25	6.01
B6	101.80	14.90	5.77
B7	98.35	12.12	6.30
B8	98.90	13.10	6.48
B9	97.23	15.42	6.57
B10	80.57	11.08	5.79
B11	80.56	11.91	5.00
B12	88.24	11.30	6.08
B13	80.86	11.21	5.34
B14	80.24	11.22	7.67
B15	80.60	10.74	5.91
B16	80.34	11.20	7.12
B17	80.63	11.01	5.33

Table 5.3: *continued*

Compound	Chemical shift of P(III)(ppm)	Chemical shift of P(V)(ppm)	Longitudinal relaxation time of P(V)(T_1,s)
B18	80.10	10.99	6.10
B19	87.79	12.23	7.55
B20	88.36	11.52	4.23
B21	88.13	12.84	5.78
B22	87.04	12.02	6.36
B23	80.07	11.38	6.34
B24	85.91	11.40	5.22
B25	80.97	10.80	6.12

Before the presentation of the results of CIDNP investigations it is very important to mention that all examined samples have had the same optical densities and therefore absorbed the same light energy. In other words if the studied compounds had the same quantum yield of the α-cleavage they would have produced the same amount of radical pairs. The optical density corresponded to the concentration 0.015 mol/l of the **M1**.

Since both cage compounds are formed by the interaction of the same pairs of radicals with the equivalent magnetic properties, CIDNP polarizations of recombination product (I_r) and disproportionation product (I_d) can be used as the estimates for the quantity of paramagnetic spices that have followed either recombination or disproportionation reactions. That is a valid assumption because all other parameters of the reacting radical pairs are the same. CIDNP polarizations are calculated from

the observed CIDNP polarizations by taking into account the longitudinal relaxation times (T_1) of the appropriate NMR transitions, *i.e* $I_r = T_1 * I_{CIDNP}$, where I_{CIDNP} is the observed CIDNP intensity of the recombination product. Measurements of relaxation times of the recombinated species were not possible because of their instability. Thus, for all MAPOs and BAPOs the relaxation times of disproportionation cage products were taken equal to 6s, what is the mean value for phosphorus nucleus in the oxidation state P(**III**). According to Turro and George[77] disproportionation cage product is formed in two photon process but in experiments with varied light energy polarization of disproportionation product was found to be linear dependent on the laser light intensity that proves single photon nature of its formation.

According to the canonic structures of the phosphinoyl radical the ratio of (I_d) and (I_r) should reflect the distribution of the unpaired electron spin between phosphorus and phosphinoyl oxygen in it. Indeed figure 5.12 shows very confident expected correlation between (I_d/I_r) and ratio of calculated overall spin densities on oxygen (D_O) and phosphorus (D_P). Moreover it demonstrates really high precision and reproducibility of the CIDNP measurements. Studied compounds are divided on the graph into four groups which generally show different efficiency in the polymerization applications. BAPOs are known to be more efficient than MAPOs, among BAPOs esters are more efficient than amides in industrial applications[78]. What is surprising, that more active compounds possess higher values of I_d/I_r. It could indicate that disproportionation reaction that was treated to be the waste one is more favorable for more active species and that more active compounds carry more spin density on oxygen than less active ones. However, the increase of I_d/I_r should be realized without the significant decrease of spin density and therefore hyperfine coupling constant (hfc) on phosphorus that would probably have led to the loss of the overall performance of photoinitiator, though QM calculations of hfcs and experimental ESR data show that there is no strait forward correlation between efficiency and hyperfine coupling constants of phosphinoyl radicals[79] (Figure 5.13). Calculated hfcs do not explain the difference in initiation efficiency of different photoinitiators, *e.g* BAPOs possess smaller hfcs but generally perform better than MAPOs. The re-

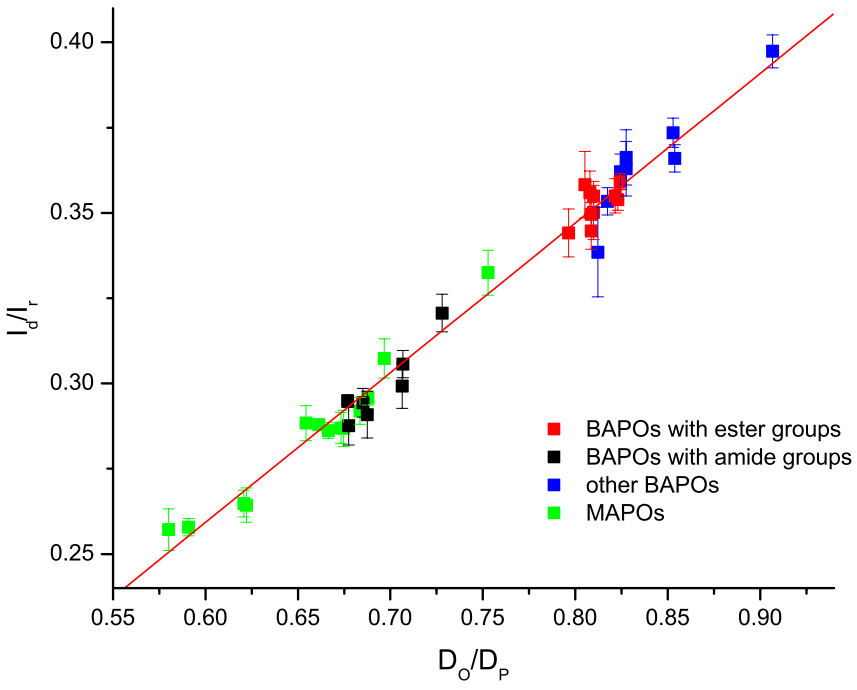

Figure 5.12: Relation between I_d/I_r and ratio of calculated overall spin densities on phosphinoyl oxygen and phosphorus.

liability of such calculations on UB3LYP/6-31G* level of theory is demonstrated on Figure 5.14 which shows that there is a very good correlation between experimental and calculated hfcs though the latter underestimate systematically values measured by ESR.

In the presence of quencher (monomer) CIDNP spectra of BAPOs and MAPOs retain only polarizations of two main cage products (I_d, I_r), the signal of escape product containing P(O)-P(O) fragment disappears what is expected because radicals escaped from the cage must have instantly reacted with the monomer. The additions of both phosphinoyl and benzoyl radicals to monomer are not observed by CIDNP since it lead to the formation of paramagnetic species (Figure 5.15).

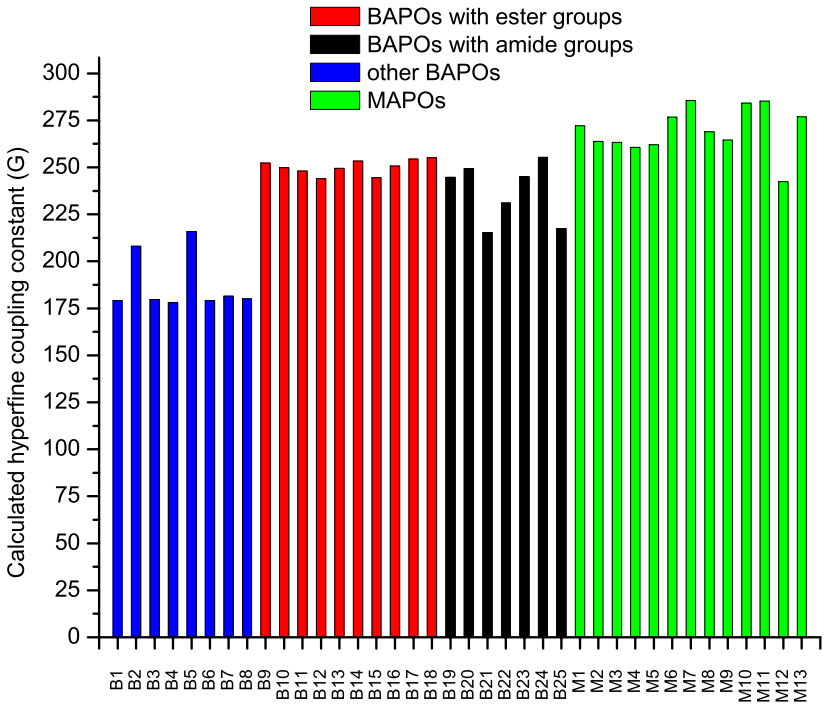

Figure 5.13: Calculated hyperfine coupling constants of compounds investigated (UB3LYP/6-31G*)

Following the changes of concentrations of both cage products by measuring theirs polarizations in the presence of quencher can theoretically tell about the number of radicals reacted with the monomer. The expected result would have been that at certain high enough quencher concentration polarizations of both cage products vanished because of the excess of monomer. At those conditions phosphinoyl radicals should react only with monomer since cage recombination and disproportionation must be very unprobable. Experimental results on **M1** are presented on Figure 5.16 which shows the dependence of the ratio of sum of cage polarizations (I_d+I_r) at certain concentration of **Q1** to the sum of polarizations at no presence of quencher (I_d^0+I_r^0) on the concentration of sterically hindered monomer **Q1**. That monomer was chosen to avoid the follow up polymerization of the reaction mixture and in-

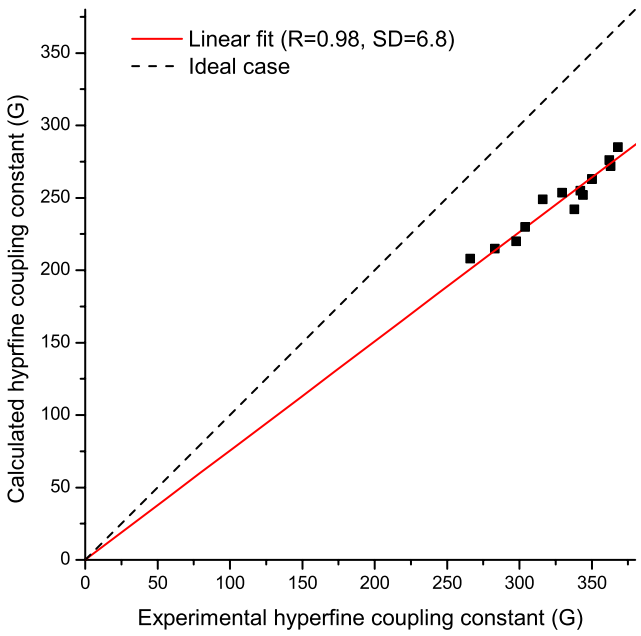

Figure 5.14: Experimental versus calculated hyperfine coupling constants of selected phosphinoyl radicals

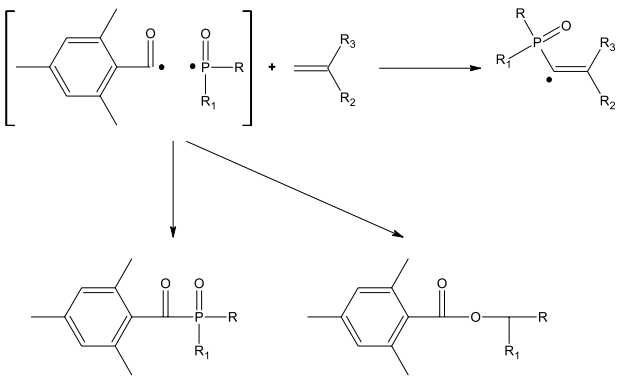

Figure 5.15: Reactions of phosphinoyl radicals in the presence of monomer

creasing of the viscosity which would have made diffusion of the reaction products very slow and significantly increase the time of the experiments.

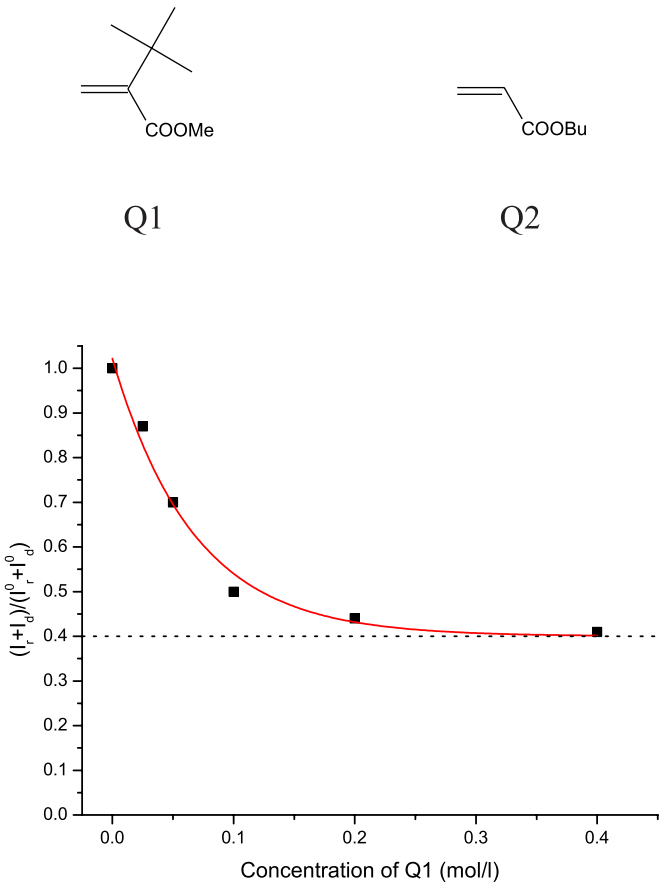

Figure 5.16: Dependence of cage polarizations of **M1** (0.015 mol/l) on the concentration of **Q1**

In contradiction to expectations experiment shows that ^{31}P-CIDNP spectra detain certain amount of polarization (about 40% of the initial polarization in the case of **M1**) even at the 16 fold excess of **Q1**. The experimental data are very well described by the exponential function of type $F(x) = y_0 + Ae^{-x/t}$, where $x = y_0$ is the asymptote of the function $F(x)$. Thus there is a certain non-zero threshold below which CIDNP polarizations do not drop down even after posterior increase of the quencher concentration. The major contribution into the value of I_d+I_r is made by I_r. I_d decreases rapidly with the increase of the monomer concentration and becomes

undetectable as is shown on Figure 5.17 already at the four fold excess of **Q1**. Species formed by the addition of phosphinoyl radical to **Q1** are very stable because

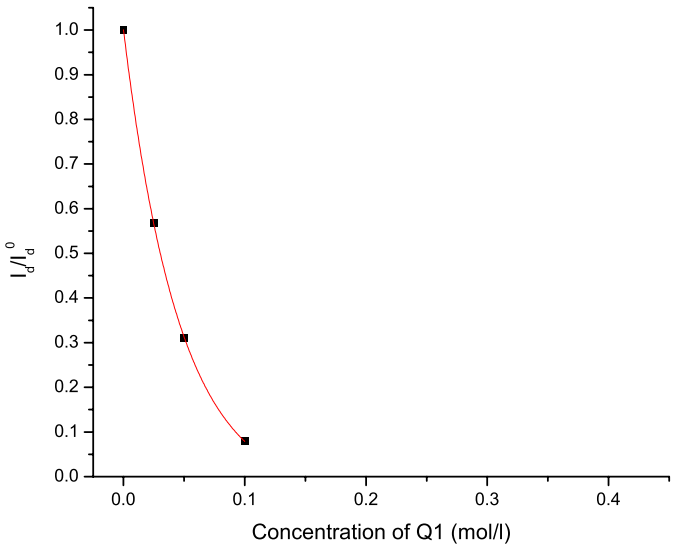

Figure 5.17: Dependence of the polarizations of disproportionation product of **M1** (0.015 mol/l) on the concentration of **Q1**

of steric hindrance of the radical center and though they do not appear in the CIDNP spectra but, in principle, can transfer polarization *via* spin-spin interactions onto the phosphorus nuclei of cage products. To reduce the probability of that the same experiments were carried out with usage of n-butylacrylate (**Q2**) instead of **Q1** since n-butylacrylate has no restrictions to react further with other molecules to produce polymer chains. The results obtained have been very the same with the slightly reduced(5-8%) residual CIDNP polarizations at the high monomer concentrations. The very final and trusty experiment to find the contribution of polarization transfer into the residual polarization of recombination products was the CIDNP experiment of the mixture of **M1** and **B2** in molar ratio 1:5 with **Q2**. In such a mixture more than 99% of 342 nm light is absorbed by **B2** resulting the predominant cleavage of the latter. If the donation of the polarization transfer into the residual CIDNP

polarization is significant the NMR signal of **M1** should have been polarized together with **B2**. However no changes of **M2** signal were detected. From that we can conclude that even if polarization transfer occurs it does not play any important role in the creation of the CIDNP enhancement and true CIDNP polarization is measured.

In above mentioned CIDNP experiments we observe polarizations from the same radical pairs under constant conditions (temperature, concentration of photoinitiator, light intensity) except for the concentration of the quencher and therefore do not change rate of singlet-triplet mixing. Based on that assumption we can suppose that according to the equation 2.13 observed polarization intensity is proportional to the number of radical pairs that have been reacted back to form parent photoinitiator. For **M1** it means that if the number of radical pairs recombined back in the absence of monomer is A then, taking into account the polarization threshold equal to 40%, we conclude that even at 20 fold excess of quencher **Q1** number of pairs recombined M is $M = 0.4A$. From Figure 5.16 follows that subsequent increase of the quencher concentration does not lead to increase of number of radical pairs reacting with monomer. Moreover, since the major contribution into the value of the residual polarization is made by recombination product (I_r) the radical pairs exhibiting higher ability to disproportionate (higher value of I_d/I_r) should possess lower polarization threshold - more phosphinoyl radicals escape from the cage and react with the monomer.

To describe non-zero asymptotic polarization phenomenon it is needed to recall that radical pair is formed in the solvent cage and its properties depend on the chemical nature of solvent, temperature and viscosity - so called cage effects. The term cage is implied hereafter as the nearest environment of the radical pair that determines its lifetime before reorientation and diffusion apart and subsequent reactions. The slow diffusion and rotation of the free radicals inside the cage would drastically increase the probability for them to react back forming initial photoinitiator. According to Noyes pair diffusion model if rotation-correlation time is two times longer than the rate of intersystem crossing it doubles the probability to find

radical pair in the singlet electron state and thus to react. On the other hand the increase of the temperature leads to the faster diffusion and finally destruction of the cage itself allowing the escape of the participating radicals. Same effect can be produced by fast compulsory mixing. The destruction of the cage should first decrease the position of asymptote and then bring it to zero. Though, the residual polarization must be a function of temperature or/and mixing. The dependence of residual polarizations on diffusion and rotation should be very pronounced especially for radicals that have bulky substituents or chemical groups that can strongly interact with the solvent molecules via non-covalent bonds.

The above mentioned argumentation must be effective for all studied MAPOs and BAPOs because of their similar chemical and magnetic properties with the only difference in the amount of the residual CIDNP polarization stored. The experimental data on the polarization threshold of recombination products are show in figure 5.18 as the function of I_d/I_r at no quencher presence. For most of the studied compounds the dependence of residual polarization on ratio between disproportionation and recombination products I_d/I_r (which can be predicted by QM calculations) is rather good. Some of the investigated object possess values that are by far not consistent with above mentioned argumentation. Those compounds carry very bulky substituents (**M7, M10, M11, M12, B2, B3, B4, B6, B8, B25**). Big substituents increasing substantially the size of the radical slow down the diffusion and reorientation of the molecules favoring the recombination. Also BAPOs with ester functional groups exhibit a bit smaller cage effect than amide derivatives. That is in a very good agreement with our hypothesis on cage dependent reactions of radical pairs. It is necessary to admit that the polarization threshold must be very dependent on the monomer used (solvation effects) and that is why the order of photoinitiators could be changed and even reversed.

5.5.2 ^{31}P-NMR

Though CIDNP gives direct information on the reacting radicals it is limited to conditions that are rather far from the real applications: quite low viscosity, rather

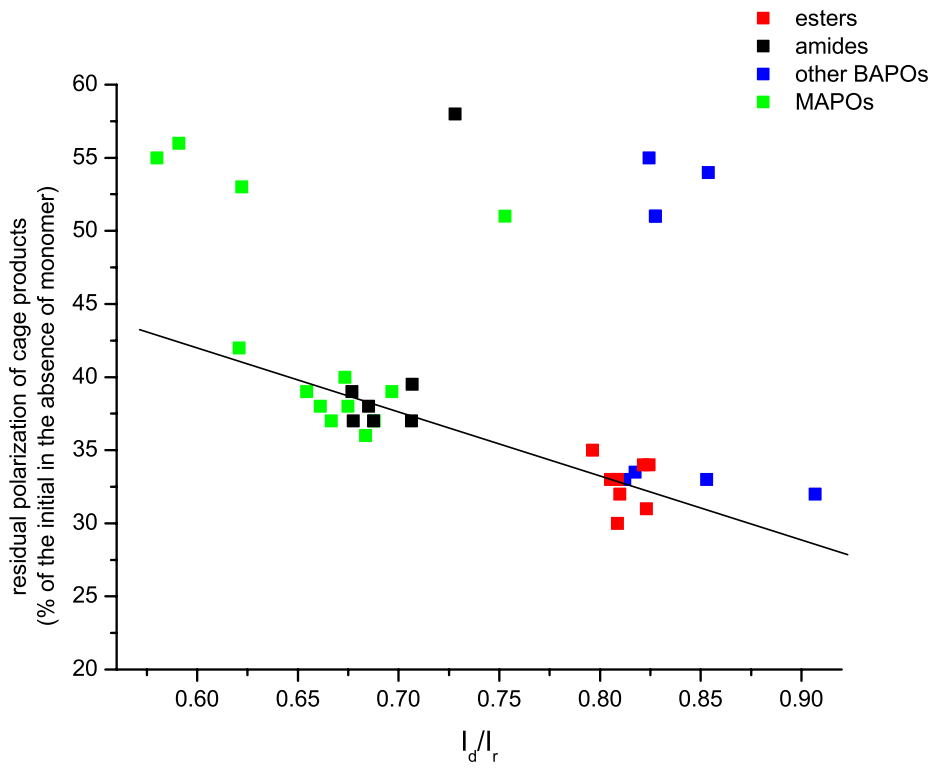

Figure 5.18: Residual polarizations of MAPOs and BAPOs investigated (0.015 mol/l) in the presence of 20 fold excess of **Q1** in % of the polarization without quencher versus I_d/I_r

high concentration of the photoinitiator and small of monomer. Those conditions are required mostly because of the small crossection of the laser beam that penetrates sample inside the CIDNP probehead allowing to generate radicals in very small volume of the NMR tube what drastically decrease sensitivity. The limitations could be overcome by the application of simple 1D NMR.

In the following experiment the very big (200 fold molar) excess of the monomer **Q2** together with the investigated photoinitiator was irradiated stepwise within the NMR tube with the excimer laser. Every step was monitored by ^{31}P-NMR. This

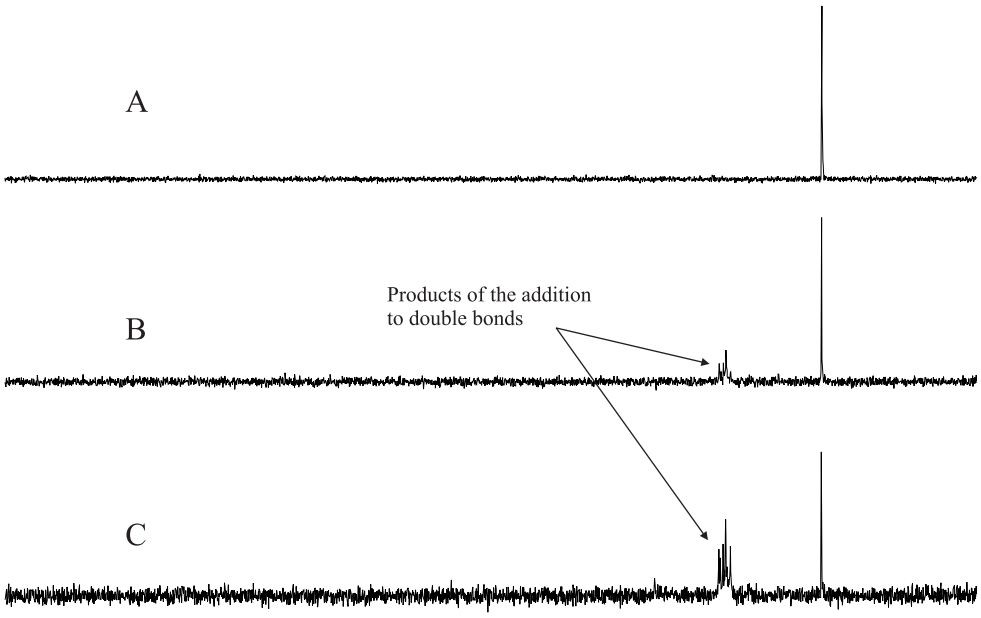

Figure 5.19: Typical NMR spectra of the phosphine oxide photoinitiator at the big excess of the monomer: A - before irradiation, B - after 10 s irradiation, C - after 20 s irradiation

technique can be easily applied to almost any monomer-photoinitiator system that contains magnetically active nuclei with the broad range of chemical shifts that do not interfere with the own monomer chemical shifts. The typical outcome is shown on figure 5.19.

The NMR transitions of ^{31}P-nuclei lie in a very broad range of about 200 ppm and are very sensitive to environment. On figure 5.19 is shown that signals of the phosphinoyl moiety added to the double bond of n-butylacrylate are easily distinguishable from those coming from all other possible phosphorus containing product. Products of the addition are represented by number of lines with the different intensities that correspond to a polymers with the different chain lengths. The simple quantitative treatment of NMR spectra provides knowledge on either relative or absolute amount of phosphinoyl radicals reacted with the monomer. Figure 5.20 presents data on the first addition (addition efficiency) of phosphinoyl radicals pro-

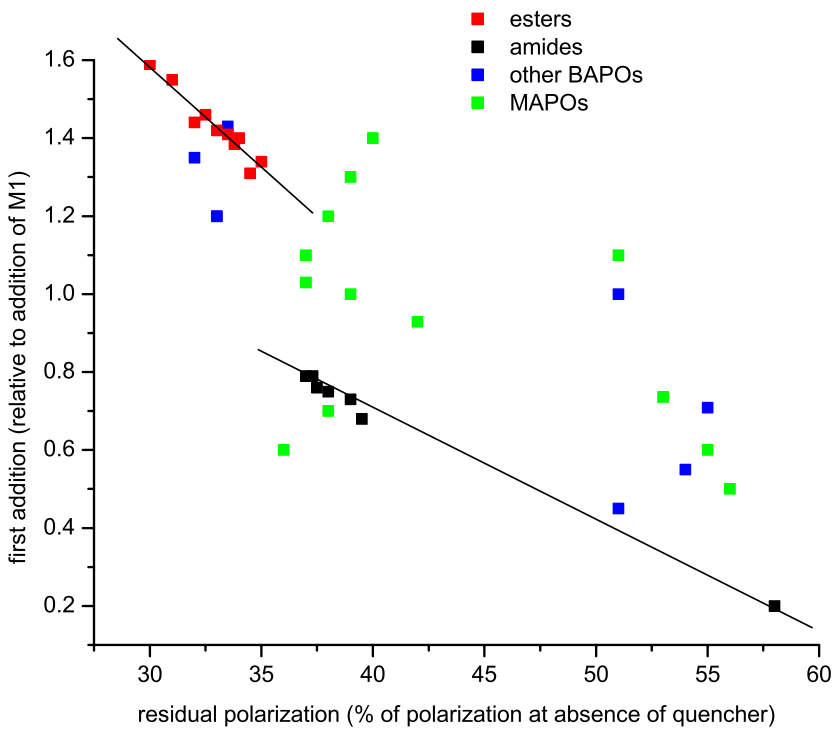

Figure 5.20: Relative addition efficiencies of ester and amide BAPOs

duced from BAPO and MAPOs to monomer **Q2**. The values measured by NMR were first reduced to the molar extinction at 308 nm and then normalized to the value for standard photoinitiator **M1** to give relative addition efficiency. Esters and amides show quite confident linear correlation between addition measured by NMR and polarization threshold of cage products obtained by ^{31}P-CIDNP bringing to the conclusion that radicals tending to disproportionate rather than recombine add to monomer better. Data of other studied MAPOs and BAPOs are distributed chaotically on the graph. The possible explanation is that within the two groups, esters and amides, compounds carrying similar chemical groups possess identical or close to each other quantum yields of α-cleavage. This is not the case for other compounds that in general belong to different chemical classes with probably very

different quantum yields.

5.6 Discussion

According to NMR experiments BAPOs possessing ester groups seem to be more efficient than amides in the first addition to the monomer. On the other hand CIDNP investigations on the ratio of disproportionation and recombination products together with QM calculations indicate that esters rather than amides prefer to perform disproportionation reaction which was thought to be the waste one. That could be explained in terms of the rate constants of particular processes taking place after photoinitiator cleavage. There are only four possible primary reactions of the

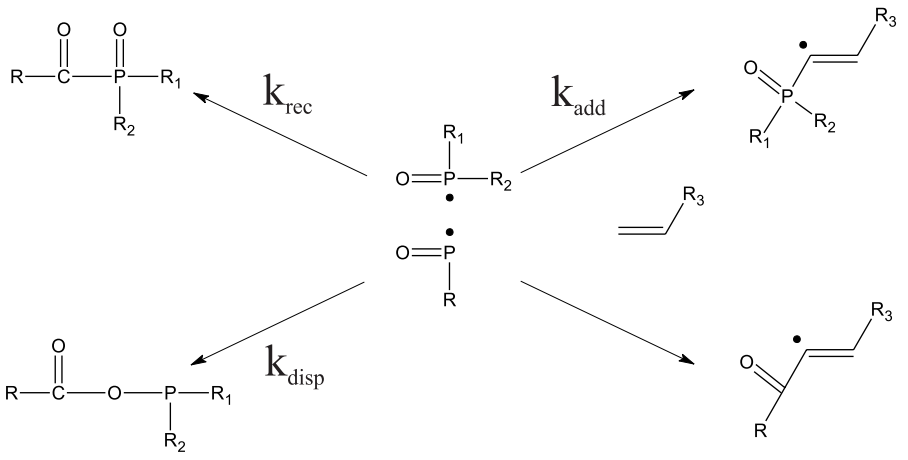

newly formed radical pair in the presence of the excess of quencher. Two cage reactions: recombination with the rate constant k_{rec} and disproportionation with the rate constant k_{disp}. Two escape: addition of phosphinoyl radical to a double bond (k_{add}) and addition of benzoyl radical. The latter is not observable by ^{31}P magnetic resonance technique. Other escape reactions that are realized in the absence of monomer are very unprobable in our case. Also the disproportionation is not detected under those conditions. It follows that addition constant of phosphinoyl radical to monomer must fulfill the following requirements: $k_{rec} > k_{add} > k_{disp}$. Since addition constants of phosphinoyl radicals are $10^7 - 10^6 M^{-1}s^{-1}$ and the polarization

itself is created in 10^{-10}s(rate of the intersystem crossing) the rate constant of recombination must lie in the range $10^9 - 10^8$ $M^{-1}s^{-1}$. The kinetic simulations that take into account diffusion, *i.e.* cage properties, are in very good agreement with those assumptions (Figure 5.21).

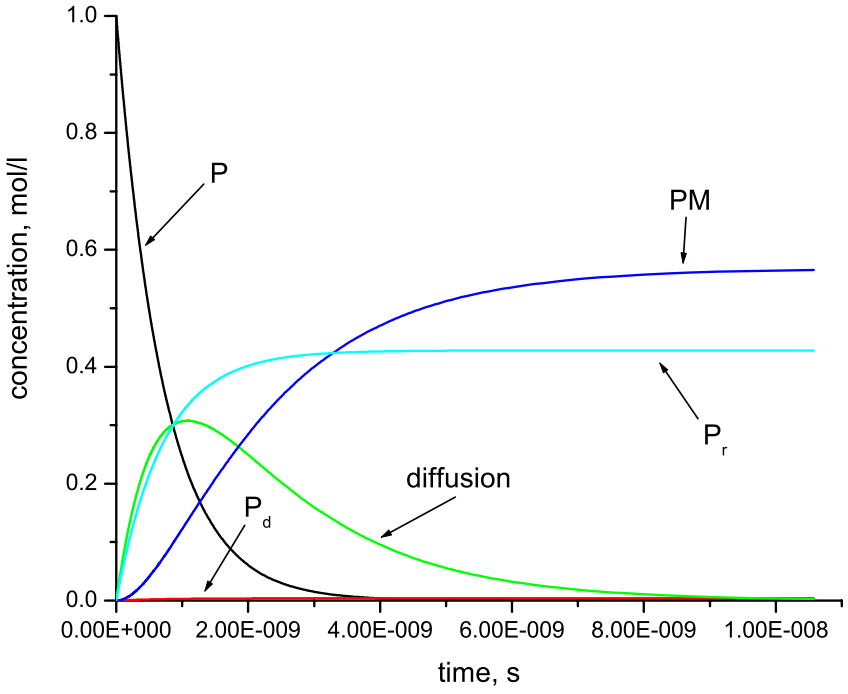

Figure 5.21: Kinetic simulation of the phosphinoyl radical reactions in the presence of 100 fold excess of the monomer. P - concentration of phosphinoyl radicals, P_r - recombination product, P_d - disproportionation product, PM - addition product. Simulation parameters - $k_{rec} = 6 \cdot 10^8$,$k_{add} = 1.9 \cdot 10^7$, $k_{disp} = 6 \cdot 10^6$, $k_{diffusion} = 8 \cdot 10^8$ M^{-1} s^{-1}

5.7 Conclusions

An extensive systematic NMR and CIDNP study on large number of similar compounds was performed. Was found a very good agreement between DFT calculations of unpaired electron overall spin densities and CIDNP data on recombination products of phosphinoyl based photoinitiators. A new NMR based method for determination of the first addition efficiency of phosphinoyl radicals is developed. Its data were found to be in excellent correlation with CIDNP measurements of polarization threshold at the conditions closed to industrial which in turn can be predicted theoretically. That can be efficiently used for theoretical predictions of efficiency and cheap industrial screening of potential photoinitiators. The results fit well to the particular kinetic model.

Chapter 6

Supplement

Curriculum Vitae

Personal information

Surname:	Neshchadin
Given name:	Dmytro
Home address:	Strassburgerallee 91, 4055 Basel
Work address:	Klingelbergstrasse 80, 4056 Basel
Phone:	+41 61 2673840
Fax:	+41 61 2673855
E-mail:	dmytro.neshchadin@unibas.ch, neshchadin@mail.ru
Date of birth:	6 May 1974
Place of birth:	Odessa (Ukraine)
Languages:	Russian, English, Ukrainian, German

Educational and working background

09/1980-05/1991	Primary and secondary school, Odessa, Ukraine
08/1991-08/1996	Mechnikov Odessa State University, Odessa, Ukraine Bogatsky Physico-Chemical Institute, National Academy of Sciences of Ukraine, Odessa, Ukraine M. Sc. Chemistry, Thesis title: "Synthesis of Macrocyclic Chromoionophores Based on Mono- and Bis-azacrown Ethers"
09/1996-02/1999	Bogatsky Physico-Chemical Institute, National Academy of Sciences of Ukraine, Odessa, Ukraine Researcher, Study of Structure-Activity Relationships of Ligands of Benzodiazepine and Dopamine Receptors
03/1999-current	Ciba Specialty Chemicals Inc., Basel, Switzerland Participant of research projects "Photophysics of free radical Cured Systems", "Photophysics of Photolatent Catalysis"
03/1999-current	University of Basel, Basel, Switzerland

Institute of Physical Chemistry
Ph.D. student
Ph.D. thesis title: "Quantitative Applications of ^{1}H and ^{31}P Chemically Induced Dynamic Nuclear Polarization"

Presentations at Conferences

03/1999	EPA Graduate Student Symposium, University of Fribourg, Switzerland - poster
08/1999	6^{th} International Symposium on Magnetic Field and Spin Effects in Chemistry, Emmeten, Switzerland - poster
02/2000	EPA Graduate Student Symposium, University of Fribourg, Switzerland - poster
10/2001	RadTech Europe, Basel, Switzerland - oral presentation
04/2002	35^{th} Annual International Meeting, Electron Spin Resonance Group, RSC, Aberdeen, UK - poster
06/2002	Workshop on Radical Ion Reactivity in Biology, Chemistry and Technology, Heigenbrücken, Germany - poster

During my study at the University of Basel I attended the lectures and courses of the following professors and lectures:
Prof. M. Jungen, Prof. B. Giese, Prof. J.P. Maier, Prof. H.-P. Huber, Prof. A.Baratoff, Prof. A.Allerton, Prof. E.Constable, Dr. O. Dopfer, Dr. G. Gescheidt, Dr. A. Shumakovitch

Scientific publications

1. Bioavailability of cinazepam during its administration as an inclusion complex with β-cyclodextrin. Andronati, S. A.; Makayan, S. Yu.; Neshchadin, D. P.; Yakubovskaya, L. N.; Sava, V. M.; Andronati, K. S., Khimiko-Farmatsevticheskii Zhurnal (1998), 32(10), 3-5.

2. 5-Phenyl- and 5-(o-chlorophenyl)-1-methyl-7-bromo-3-hydroxy-1,3-dihydro-2H-1,4-benzodiazepin-2-ones and their inclusion complexes with benzene. Andronati, S. A.; Andronati, K. S.; Neschadin, D. P.; Simonov, Yu. A.; Kravtsov, V. Kh.; Lipkowsky, J., Dopovidi Natsional'noi Akademii Nauk Ukraini (1999), (6), 149-155.

3. M. Kunz, K. Dietliker, J.P. Wolf, I. Gatlik, D. Neshchadin, U. Buser, G. Rist, G. Gescheidt, STZ Technik 7-8(1999), 14.

4. σ-Bishomoconjugation (s-bishomoaromaticity) in 4C/3(2)e cations - scope and limitations. Prinzbach, Horst; Reinbold, Jens; Bertau, Martin; Voss, Torsten; Martin, Hans-Dieter; Mayer, Bernhard; Heinze, Jurgen; Neschchadin, Dmytro; Gescheidt, Georg; Prakash, G. K. Surya; Olah, George A. , Angewandte Chemie, International Edition (2001), 40(5), 911-914.

5. Secododecahedradienes - syntheses, reactivity, in-plane homoconjugated 3C/2e cations, 4C/3e radical cations, and σ-bishomoaromatic 4C/2e dications? Reinbold, Jens; Bertau, Martin; Voss, Torsten; Hunkler, Dieter; Knothe, Lothar; Prinzbach, Horst; Neschchadin, Dmytro; Gescheidt, Georg; Mayer, Bernhard; Martin, Hans-Dieter; Heinze, Jurgen; Prakash, G. K. Surya; Olah, George A. Helvetica Chimica Acta (2001), 84(6), 1518-1560.

6. Spectroscopic Investigations of Bis(sulfoximine) Copper(II) Complexes and Their Relevance in Asymmetric Catalysis. Bolm, Carsten; Martin, Marc; Gescheidt, Georg; Palivan, Cornelia; Neshchadin, Dmytro; Bertagnolli, Helmut; Feth, Martin; Schweiger, Arthur; Mitrikas, George; Harmer, Jeffrey, Journal of the American Chemical Society (2003), 125(20), 6222-6227.

7. Stereocontrolled photo-reaction pathways of endo/exo-2-benzoyl-substituted bicyclo[2.2.2]oct-5-en-2-ol: Paterno-Buechi reaction versus α-cleavage. Gescheidt, G.; Neshchadin, D.; Rist, G.; Borer, A.; Dietliker, K.; Misteli, K., Physical Chemistry Chemical Physics (2003), 5(6), 1071-1077.

Bibliography

[1] Kaptein, R.; Oosterhoff, L. J. *Chemical Physics Letters* **1969**, *4*(4), 195–7.

[2] Kaptein, R.; Oosterhoff, L. J. *Chemical Physics Letters* **1969**, *4*(4), 214–16.

[3] Closs, G. L. *Journal of the American Chemical Society* **1969**, *91*(16), 4552–4.

[4] Closs, G. L.; Trifunac, A. D. *Journal of the American Chemical Society* **1970**, *92*(7), 2183–4.

[5] Closs, G. L.; Trifunac, A. D. *Journal of the American Chemical Society* **1970**, *92*(7), 2186–7.

[6] Lepley, A. R.; Closs, G. L.; Editors. *Chemically Induced Magnetic Polarization;* 1973.

[7] Muus, L. T.; Atkins, P. W.; McLauchlan, K. A.; Pedersen, J. B.; Editors. *NATO Advanced Study Institute Series, Vol. C34: Chemically Induced Magnetic Polarization;* 1977.

[8] Pedersen, J. B. *Theories of Chemically Induced Magnetic Polarization;* 1979.

[9] Kaptein, R. *Advances in Free-Radical Chemistry (London)* **1975**, *5*, 319–80.

[10] Bagryanskaya, E. G.; Sagdeev, R. Z. *Russian Chemical Reviews* **2000**, *69*(11), 925–945.

[11] Pine, S. H. *Journal of Chemical Education* **1972**, *49*(10), 664–8.

[12] Goez, M. *Concepts in Magnetic Resonance* **1995**, *7*(4), 263–79.

[13] Azumi, T. *Dynamic Spin Chemistry* **1998**, pages 153–186.

[14] Freed, J. H.; Pedersen, J. B. *Advances in Magnetic Resonance* **1976**, *8*, 1–84.

[15] Closs, G. L. *Advances in Magnetic Resonance* **1974**, *7*, 157–229.

[16] Goez, M. *Journal of Information Recording* **1998**, *24*(1-2), 9–22.

[17] Goez, M. *Concepts in Magnetic Resonance* **1995**, *7*(1), 69–86.

[18] Goez, M. *Concepts in Magnetic Resonance* **1995**, *7*(2), 137–52.

[19] Lawler, R. G. *Accounts of Chemical Research* **1972**, *5*(1), 25–33.

[20] Ward, H. R. *Accounts of Chemical Research* **1972**, *5*(1), 18–24.

[21] Slichter, C. P. *Principles of Magnetic Resonance. 2nd Ed;* 1978.

[22] Kaptein, R. *Journal of the Chemical Society [Section] D: Chemical Communications* **1971**, (14), 732–3.

[23] Adrian, F. J. *Journal of Chemical Physics* **1970**, *53*(8), 3374–5.

[24] Kaptein, R. *Journal of the American Chemical Society* **1972**, *94*(18), 6251–62.

[25] Toriyama, K.; Nunome, K.; Iwasaki, M.; Shida, T.; Ushida, K. *Chemical Physics Letters* **1985**, *122*(1-2), 118–23.

[26] Ohta, K.; Nakatsuji, H.; Kubodera, H.; Shida, T. *Chemical Physics* **1983**, *76*(2), 271–81.

[27] Shida, T.; Egawa, Y.; Kubodera, H.; Kato, T. *Journal of Chemical Physics* **1980**, *73*(12), 5963–70.

[28] Dewar, M. J. S.; Merz, Kenneth M., J. *Theochem* **1985**, *23*(1-2), 59–65.

[29] McKee, M. L.; Radom, L. *Organic Mass Spectrometry* **1993**, *28*(10), 1238–44.

[30] Jungwirth, P.; Bally, T. *Journal of the American Chemical Society* **1993**, *115*(13), 5783–9.

[31] Bouma, W. J.; Poppinger, D.; Radom, L. *Theochem* **1983**, *12*, 209–18.

[32] Woodward, R. B.; Hoffmann, R. *Angewandte Chemie, International Edition in English* **1969**, *8*(11), 781–853.

[33] Prinzbach, H.; Wollenweber, M.; Herges, R.; Neumann, H.; Gescheidt, G.; Schmidlin, R. *Journal of the American Chemical Society* **1995**, *117*(4), 1439–40.

[34] Jungwirth, P.; Carsky, P.; Bally, T. *Journal of the American Chemical Society* **1993**, *115*(13), 5776–82.

[35] Etzkorn, M.; Wahl, F.; Keller, M.; Prinzbach, H.; Barbosa, F.; Peron, V.; Gescheidt, G.; Heinze, J.; Herges, R. *Journal of Organic Chemistry* **1998**, *63*(18), 6080–6081.

[36] Fessner, W. D.; Murty, B. A. R. C.; Prinzbach, H. *Angewandte Chemie* **1987**, *99*(5), 482–4.

[37] Fessner, W. D.; Murty, B. A. R. C.; Woerth, J.; Hunkler, D.; Fritz, H.; Prinzbach, H.; Roth, W. D.; Schleyer, P. v. R.; McEwen, A. B.; Maier, W. F. *Angewandte Chemie* **1987**, *99*(5), 484–6.

[38] Prinzbach, H.; Weber, K. *Angewandte Chemie* **1994**, *106*(22), 2329–48 (See also Angew. Chem., Int. Ed. Engl., 1994, 33(22), 2239–57).

[39] Exner, K. PhD thesis, Freiburg University (Germany), **2000**.

[40] Etzkorn, M. *Homologous (Iso)Pagodanes and (Iso)Pagodadienes - Syntheses, 4C/3e Radical Cations and 4C/2e Dications* PhD thesis, Freiburg University (Germany), **1998**.

[41] Akkermans, R. P.; Suarez, M. F.; Roberts, S. L.; Fulian, Q.; Compton, R. G. *Electroanalysis* **1999**, *11*(16), 1191–1202.

[42] Abelt, C. J.; Roth, H. D. *Journal of the American Chemical Society* **1986**, *108*(21), 6734–9.

[43] Roth, H. D.; Abelt, C. J. *Journal of the American Chemical Society* **1986**, *108*(8), 2013–19.

[44] Roth, H. D.; Herbertz, T.; Lakkaraju, P. S.; Sluggett, G.; Turro, N. J. *Journal of Physical Chemistry A* **1999**, *103*(51), 11350–11354.

[45] Roth, H. D.; Weng, H.; Herbertz, T. *Tetrahedron* **1997**, *53*(29), 10051–10070.

[46] Blois, M. S., J.; Braun, H. W.; Maling, J. E. *Arch. Sci. Geneva* **1960**, *13*(Spec. No.), 243–55.

[47] Prinzbach, H.; Murty, B. A. R. C.; Fessner, W. D.; Mortensen, J.; Heinze, J.; Gescheidt, G.; Gerson, F. *Angewandte Chemie* **1987**, *99*(5), 488–90.

[48] Gescheidt, G.; Prinzbach, H.; Davies, A. G.; Herges, R. *Acta Chemica Scandinavica* **1997**, *51*(2), 174–180.

[49] Prinzbach, H.; Reinbold, J.; Bertau, M.; Voss, T.; Martin, H.-D.; Mayer, B.; Heinze, J.; Neschchadin, D.; Gescheidt, G.; Prakash, G. K. S.; Olah, G. A. *Angewandte Chemie, International Edition* **2001**, *40*(5), 911–914.

[50] Reinbold, J.; Bertau, M.; Voss, T.; Hunkler, D.; Knothe, L.; Prinzbach, H.; Neschchadin, D.; Gescheidt, G.; Mayer, B.; Martin, H.-D.; Heinze, J.; Prakash, G. K. S.; Olah, G. A. *Helvetica Chimica Acta* **2001**, *84*(6), 1518–1560.

[51] Gescheidt, G.; Herges, R.; Neumann, H.; Heinze, J.; Wollenweber, M.; Etzkorn, M.; Prinzbach, H. *Angewandte Chemie, International Edition in English* **1995**, *34*(9), 1016–19.

[52] Weber, K.; Lutz, G.; Knothe, L.; Mortensen, J.; Heinze, J.; Prinzbach, H. *Journal of the Chemical Society, Perkin Transactions 2: Physical Organic Chemistry* **1995**, (11), 1991–7.

[53] Trifunac, A. D.; Werst, D. W.; Herges, R.; Neumann, H.; Prinzbach, H.; Etzkorn, M. *Journal of the American Chemical Society* **1996**, *118*(39), 9444–9445.

[54] Roth, H. D. *Accounts of Chemical Research* **1977**, *10*(3), 85–91.

[55] Roth, H. D.; Schilling, M. L. M.; Hutton, R. S.; Truesdale, E. A. *Journal of the American Chemical Society* **1983**, *105*(2), 153–7.

[56] Roth, H. D.; Schilling, M. L. M.; Raghavachari, K. *Journal of the American Chemical Society* **1984**, *106*(1), 253–5.

[57] Prinzbach, H.; Gescheidt, G.; Martin, H. D.; Herges, R.; Heinze, J.; Surya Prakash, G. K.; Olah, G. A. *Pure and Applied Chemistry* **1995**, *67*(5), 673–82.

[58] Acylphosphine compounds and their use. Henne, A.; Hesse, A.; Jacobi, M.; Wallbillich, G.; Bronstert, B. **1982**.

[59] Baxter, J. E.; Davidson, R. S.; Hageman, H. J.; Overeem, T. *Makromolekulare Chemie, Rapid Communications* **1987**, *8*(6), 311–14.

[60] Kamachi, M.; Kuwata, K.; Sumiyoshi, T.; Schnabel, W. *Journal of the Chemical Society, Perkin Transactions 2: Physical Organic Chemistry (1972-1999)* **1988**, (6), 961–5.

[61] Sumiyoshi, T.; Schnabel, W. *Makromolekulare Chemie* **1985**, *186*(9), 1811–23.

[62] Sumiyoshi, T.; Schnabel, W.; Henne, A. *Journal of Photochemistry* **1985**, *30*(1), 63–80.

[63] Schnabel, W.; Sumiyoshi, T. *New Trends Photochem. Polym., [Proc. Int. Symp. Honour Professor Bengt Raanby]* **1985**, pages 69–83.

[64] Sumiyoshi, T.; Schnabel, W.; Henne, A.; Lechtken, P. *Polymer* **1985**, *26*(1), 141–6.

[65] Baxter, J. E. *Acylphosphine oxides as photoinitiators* PhD thesis, **1988**.

[66] Baxter, J. E.; Davidson, R. S.; Hageman, H. J. *Polymer* **1988**, *29*(9), 1569–74.

[67] Gescheidt, G.; Hristova, U. r. *Unpublished results* **2003**.

[68] Kolczak, U.; Rist, G.; Dietliker, K.; Wirz, J. *Journal of the American Chemical Society* **1996**, *118*(27), 6477–6489.

[69] Kajiwara, A.; Konishi, Y.; Morishima, Y.; Schnabel, W.; Kuwata, K.; Kamachi, M. *Macromolecules* **1993**, *26*(7), 1656–8.

[70] Weber, M.; Khudyakov, I. V.; Turro, N. J. *Journal of Physical Chemistry A* **2002**, *106*(10), 1938–1945.

[71] Jockusch, S.; Turro, N. J. *Book of Abstracts, 216th ACS National Meeting, Boston, August 23-27* **1998**, pages PHYS–291.

[72] Gatlik, I.; Rzadek, P.; Gescheidt, G.; Rist, G.; Hellrung, B.; Wirz, J.; Dietliker, K.; Hug, G.; Kunz, M.; Wolf, J.-P. *Journal of the American Chemical Society* **1999**, *121*(36), 8332–8336.

[73] Khudyakov, I. V.; Weber, M.; Turro, N. J. *Abstracts of Papers, 222nd ACS National Meeting, Chicago, IL, United States, August 26-30, 2001* **2001**, pages POLY–366.

[74] Weber, M.; Turro, N. J. *Journal of Physical Chemistry A* **2003**, *107*(18), 3326–3334.

[75] Spichty, M.; Turro, N. J.; Rist, G.; Birbaum, J. L.; Dietliker, K.; Wolf, J. P.; Gescheidt, G. *Journal of Photochemistry and Photobiology, A: Chemistry* **2001**, *142*(2-3), 209–213.

[76] Khudyakov, I. V.; Arsu, N.; Jockusch, S.; Turro, N. J. *Designed Monomers and Polymers* **2003**, *6*(1), 91–101.

[77] Turro, N. J.; George, M. P. c. **2002**.

[78] Personal communication. Wolf, J. P. CIBA SC, **2002**.

[79] Gatlik, I. *Time-Resolved ESR investigation of photoinitiators for radical induced polymerisation* PhD thesis, University of Basel, **2001**.